

AD722345

NOLTR 71-5

NOL HYPERVELOCITY WIND TUNNEL
REPORT NO. 1: AERODYNAMIC DESIGN

By
E. L. Harris
W. J. Glowacki

26 FEBRUARY 1971

NOL

NAVAL ORDNANCE LABORATORY, WHITE OAK, SILVER SPRING, MARYLAND

NOLTR 71-5

ATTENTION

This document has been approved for
public release and sale, its distribution
is unlimited.

DDC
RECEIVED
APR 29 1971
REGISTRY
C

UNCLASSIFIED

Security Classification

DOCUMENT CONTROL DATA - R & D

(Security classification of title, body of abstract and indexing annotation must be entered when the overall report is classified)

| | | | |
|---|--|---|-----------------------|
| 1. ORIGINATING ACTIVITY (Corporate author) Naval Ordnance Laboratory Silver Spring, Maryland 20910 | | 2a. REPORT SECURITY CLASSIFICATION UNCLASSIFIED | |
| | | 2b. GROUP N/A | |
| 3. REPORT TITLE NOL HYPERVELOCITY WIND TUNNEL, REPORT NO. 1: AERODYNAMIC DESIGN | | | |
| 4. DESCRIPTIVE NOTES (Type of report and inclusive dates) | | | |
| 5. AUTHOR(S) (First name, middle initial, last name) E. Leroy Harris. Walter J. Glowacki | | | |
| 6. REPORT DATE 26 February 1971 | | 7a. TOTAL NO. OF PAGES 58 | 7b. NO. OF REFS 15 |
| 8a. CONTRACT OR GRANT NO. | | 9a. ORIGINATOR'S REPORT NUMBER(S) NOLTR 71-5 | |
| b. PROJECT NO. | | | |
| c. | | 9b. OTHER REPORT NO(S) (Any other numbers that may be assigned this report) | |
| d. | | | |
| 10. DISTRIBUTION STATEMENT This document has been approved for public release and sale, its distribution is unlimited. | | | |
| 11. SUPPLEMENTARY NOTES | | 12. SPONSORING MILITARY ACTIVITY | |
| | | | |
| 13. ABSTRACT The NOL Hypervelocity Wind Tunnel will provide a high Reynolds number turbulent flow simulation in the Mach number range 10 to 20. This facility, much needed for large-scale testing of hypersonic vehicles, is under construction and will be operational late in 1972. Supply pressures up to 40,000 psi will be maintained constant for 1 to 4 seconds during which stable, condensation-free flow conditions will prevail. Very high Reynolds numbers, ranging from 6.5×10^6 at Mach number 20 to 46×10^6 at Mach number 10 (based on the five-foot nozzle exit diameter), are obtained by operating with nitrogen at temperatures just sufficient to avoid test section condensation. The facility, which operates in a blowdown mode, has separate legs for the three design Mach numbers 10, 15, and 20. Each leg is fitted with its own storage heater, diaphragm assembly, contoured nozzle, and diffuser. The three legs share a common gas storage supply, test cell and model support system, and vacuum sphere. This report will highlight the more significant considerations leading to the aerodynamic design of the facility and will include discussions of the need for the facility, the initial requirements imposed on its design, and brief descriptions of the layout and operation of the facility. | | | |

UNCLASSIFIED

Security Classification

| 14 KEY WORDS | LINK A | | LINK B | | LINK C | |
|---|--------|----|--------|----|--------|----|
| | ROLE | WT | ROLE | WT | ROLE | WT |
| Hypervelocity Wind tunnel Aerodynamic design Nozzles | | | | | | |

UNCLASSIFIED

NOLTR 71- 5

NOL HYPERVELOCITY WIND TUNNEL
Report No. 1: Aerodynamic Design

Prepared by:
E. L. Harris
W. J. Glowacki

ABSTRACT: The NOL Hypervelocity Wind Tunnel will provide a high Reynolds number turbulent flow simulation in the Mach number range 10 to 20. This facility, much needed for large-scale testing of hypersonic vehicles, is under construction and will be operational late in 1972. Supply pressures up to 40,000 psi will be maintained constant for 1 to 4 seconds during which stable, condensation-free flow conditions will prevail. Very high Reynolds numbers, ranging from 6.5×10^6 at Mach number 20 to 46×10^6 at Mach number 10 (based on the five foot nozzle exit diameter), are obtained by operating with nitrogen at temperatures just sufficient to avoid test section condensation. The facility, which operates in a blowdown mode, has separate legs for the three design Mach numbers 10, 15, and 20. Each leg is fitted with its own storage heater, diaphragm assembly, contoured nozzle, and diffuser. The three legs share a common gas storage supply, test cell and model support system, and vacuum sphere. This report will highlight the more significant considerations leading to the aerodynamic design of the facility and will include discussions of the need for the facility, the initial requirements imposed on its design, and brief descriptions of the layout and operation of the facility.

U. S. NAVAL ORDNANCE LABORATORY
WHITE OAK, MARYLAND

i
UNCLASSIFIED

NOLTR 71-5

26 February 1971

NOL HYPERVELOCITY WIND TUNNEL REPORT NO. 1: AERODYNAMIC DESIGN

This report is the first of a series of technical reports describing the design and performance of the NOL Hypervelocity Wind Tunnel. The present report describes the facility and its mode of operation in very general terms and summarizes the more significant aspects of the aerodynamic design of the facility. Future reports in the series will include more detailed descriptions of individual design features or calculation methods used in the development of the facility. Tunnel performance and test results will be reported when available.

The development of the Hypervelocity Wind Tunnel has required the dedicated effort of many NOL personnel over a period of many years. It is this combined effort which has made this unique and valuable facility possible.

GEORGE G. BALL
Captain, USN
Commander

L. H. Schindel
L. H. SCHINDEL
By direction

CONTENTS

| | <u>Page</u> |
|---|-------------|
| INTRODUCTION | 1 |
| WIND TUNNEL OPERATION | 3 |
| General Description and Method of Operation | 3 |
| Pressure and Temperature Changes in the Heater Vessel | 4 |
| Pressure and Temperature Changes in the Vacuum Sphere | 10 |
| PROPERTIES OF HIGH-DENSITY NITROGEN | 12 |
| Thermodynamic Properties | 12 |
| Condensation Line Properties | 14 |
| Viscosity | 15 |
| NOZZLE DESIGN | 17 |
| Nozzle Supply and Test Conditions | 17 |
| Inviscid Core | 18 |
| Boundary Layer | 19 |
| Nozzle Dimensions | 20 |
| CONCLUDING REMARKS | 21 |
| REFERENCES | 22 |

TABLES

| Table | Title |
|-------|--|
| 1 | Nitrogen Properties at Condensation Threshold |
| 2 | Nozzle Supply and Test Section Conditions |
| 3 | Selected Inviscid Core and Nozzle Wall Coordinates |
| 4 | Selected Nozzle Dimensions |

ILLUSTRATIONS

| Figure | Title |
|--------|--|
| 1 | Comparison of Free-Flight Reynolds Numbers with those Available in the Facility |
| 2 | Required Supply Pressure, Core Diameter, and Volume Flow Rate for given Re_{DC} and Mass Flow Rate (Mach 10) |
| 3 | Required Supply Pressure, Core Diameter, and Volume Flow Rate for given Re_{DC} and Mass Flow Rate (Mach 15) |
| 4 | Required Supply Pressure, Core Diameter, and Volume Flow Rate for given Re_{DC} and Mass Flow Rate (Mach 20) |
| 5 | Cutaway View of Tunnel System |
| 6 | Variation of Isentropic Exponent with Pressure and Temperature |
| 7 | Ratio of Temperature Changes to Pressure Changes in Heater Vessel During Run with Open-Closed Type Valves. |
| 8 | Pressure Rise in Vacuum Sphere During Tunnel Operation |
| 9 | Temperature Rise in Vacuum Sphere During Tunnel Operation |
| 10 | Comparison of Pressure-Temperature Variations at High Densities with AEDC Data Tabulations |
| 11 | Variation of Reynolds Number in Test Section with Temperature for Constant Pressure or Condensation Threshold Operation at Mach 20 |
| 12 | Variation of Pressure in Test Section with Temperature for Condensation Threshold Operation |
| 13 | Variation of Density in Test Section with Temperature for Condensation Threshold Operation |
| 14 | Variation of Entropy in Test Section with Temperature for Condensation Threshold Operation |
| 15 | Variation of Enthalpy in Test Section with Temperature for Condensation Threshold Operation |

ILLUSTRATIONS (Cont.)

Figure

- 16 Variation of Sound Speed in Test Section with Temperature for Condensation Threshold Operation
- 17 Variation of Mass Flow in Test Section with Temperature for Condensation Threshold Operation
- 18 Variation of Reynolds Number in Test Section with Temperature for Condensation Threshold Operation
- 19 Variation of Viscosity in Test Section with Temperature for Condensation Threshold Operation
- 20 Variation of Supply Pressure Required for Condensation Threshold Operation with Test Section Temperature and Mach Number
- 21 Variation of Supply Temperature Required for Condensation Threshold Operation with Test Section Temperature and Mach Number
- 22 Variation of Supply Density Required for Condensation Threshold Operation with Test Section Temperature and Mach Number
- 23 Schematic Diagram of Nozzle Exit Showing Definition and Location of Optimum Cutoff Point

List of Symbols

| | |
|----------------------------|---|
| a | Sound speed |
| A | Nozzle cross-sectional area |
| B' | Constant in compressibility equation (19) |
| C _p | Specific heat at constant pressure |
| C' | Constant in compressibility equation (19) |
| d | Diameter |
| E | Internal energy per unit mass |
| g | Acceleration due to gravity |
| h | Height of heater |
| H | Enthalpy |
| L | Length |
| m | Mass |
| M | Mach Number |
| p | Pressure |
| Q | Heat |
| R | Gas Constant |
| Re | Reynolds Number |
| S | Entropy |
| t | Time |
| T | Temperature |
| T _R | Reduced temperature, equation (23) |
| T* | Reduced temperature, equation (22) |
| u | Flow velocity |
| V | Volume |
| x | Distance from throat along nozzle axis |
| Z | Compressibility factor |
| γ | Ratio of specific heats |
| γ _E | Isentropic exponent, equation (6) |
| δ | Boundary layer thickness |
| δ* | Boundary layer displacement thickness |
| μ | Viscosity |
| μ _{T_c} | Viscosity at critical temperature |
| ρ | Density |
| τ | Time scale of interest |
| Ω (2,2)* | Collision integral, equation (22) |

Subscripts

| | |
|---|----------------|
| a | In hot gas |
| b | In cold gas |
| e | At nozzle exit |

List of Symbols (Cont.)

| | |
|----------------|----------------------|
| i | Initial |
| T _c | Critical temperature |
| TG | Test gas |
| o | Supply |
| * | At nozzle throat |

Superscripts

| | |
|-----|---------|
| (i) | Initial |
| (f) | Final |

INTRODUCTION

This report summarizes the aerodynamic design of a new hyper-velocity wind tunnel currently being installed at the U. S. Naval Ordnance Laboratory (NOL). The wind tunnel is being built using military construction funds appropriated by the U. S. Congress in fiscal year 1967. It will be completed in calendar year 1972. The Mach number range is from 10 to 20 at Reynolds numbers as high as possible using nitrogen gas heated just enough to avoid condensation in the test section. The tunnel operates in a blowdown mode with a minimum running time of one second.

The emphasis in the new facility is on achieving high Reynolds numbers along with the high Mach numbers to allow testing under conditions of low altitude-high velocity flight. Figure 1 is a graph of the Reynolds number per foot variation in the earth's atmosphere as a function of altitude and Mach number. For illustrative purposes, the trajectory of an IRBM and ICBM having ballistic coefficients of 1000 lb/ft^2 has been superimposed on the figure. One sees that the Reynolds numbers become exceedingly high at low altitude and high Mach numbers, higher than can be duplicated in a wind tunnel. However, one can go a long way toward achieving an adequate testing capability in this high Reynolds number, high Mach number regime by ensuring a turbulent boundary layer. This is because laminar and turbulent boundary layers are essentially different and one can only hope to extrapolate turbulent data to higher Reynolds numbers if the boundary layer is already turbulent. Hence, in the present facility, we are striving to produce a turbulent boundary layer at all Mach numbers. At Mach number 20, the possibility of doing so is marginal - at Mach numbers 10 and 15 the boundary layers will be turbulent.

One may well ask why it is necessary to have a high Mach number, high Reynolds number facility when re-entry vehicles are already flying successfully at Mach numbers of about 20 with turbulent boundary layers. The answer is that these are vehicles of rather simple shapes which have been designed successfully after considerable free-flight testing. With better ground test facilities to simulate

the fluid mechanics, one can expect to reduce the amount of free-flight testing considerably. Also, we expect more sophisticated shapes such as maneuverable re-entry bodies to evolve over the next decade, and we will want to test these shapes under conditions which closely approximate those that occur in flight. It is very easy to compile a list of fluid dynamic flow phenomena which are not understood in a general sense, and hence we require either more research to understand them and/or developmental testing as needed to make sure the phenomena are being handled adequately for a particular vehicle. Here is a partial list.

- (1) boundary layer separation phenomena and their influence on control effectiveness,
- (2) turbulent boundary layer behavior at high Mach numbers,
- (3) boundary layer transition,
- (4) aerodynamic forces on general shapes and control surfaces,
- (5) effects of nose bluntness on vehicle stability and control effectiveness at high Mach numbers,
- (6) turbulent wakes, especially at high Mach numbers.

In the initial thinking for this wind tunnel, we set down four requirements:

- (1) Mach numbers from 10 to 20,
- (2) test duration of at least one second,
- (3) ability to create turbulent boundary layers on models at Mach 10 and 15 with a Reynolds number as high as possible at Mach 20,
- (4) test section diameter of at least three feet.

Before proceeding further, it is worthwhile to examine Figures 2, 3, and 4 which are based on information to be developed later in this report. These figures were calculated on the basis of an inviscid flow and an isentropic expansion from the supply conditions to the test conditions. The test conditions were taken to be at the condensation threshold of nitrogen. Figures 2, 3, and 4 were used in the initial phases of the tunnel design in order to choose suitable nozzle dimensions and supply conditions based on Reynolds number, volume flow rates, size and pressure. It is apparent from the figures that high Reynolds numbers may be achieved by operating large

nozzles at high supply pressures. However, this also requires large mass flow and volume flow rates - that is, large heater volumes to achieve a one-second run time. The three nozzle sizes which were finally arrived at are indicated on the figures. They have been chosen to have the same physical exit diameter of five feet when the boundary layer correction is included. The accompanying table summarizes the important nozzle parameters; this information is presented in this part of the report because it is believed that these numbers will make the rest of the report more readable.

| | Mach Number | | |
|--|------------------|------------------|-------------------|
| | 10 | 15 | 20 |
| Nozzle throat dia. d_* (in.) | 2.40 | .89 | .33 |
| Nozzle exit dia. d_e (ft.) | 5.0 | 5.0 | 5.0 |
| Supply pressure p_o (atm.) | 430 | 2365 | 3110 |
| Supply temperature T_o ($^{\circ}$ R) | 1854 | 3317 | 5040 |
| Exit displacement thickness δ_e^* (ft.) | .31 | .48 | .75 |
| Nozzle length (ft.) | 40 | 40 | 40 |
| Reynolds No. based on d_e , Re_{d_e} | 46×10^6 | 30×10^6 | 6.5×10^6 |

With the above information as background, we will discuss in more detail some of the aerodynamic information on which the wind tunnel is based. We will not discuss the mechanical details other than to state that some rather sophisticated high pressure vessel design has been necessary. No discussion of the heater will be given except in a conceptual sense in the next section. Further details on the mechanical design of the facility are included in reference (1). We intended this report to be the first of a series on the NOL Hypervelocity Wind Tunnel. Other reports will treat particular aspects of the tunnel in more detail.

Wind Tunnel Operation

General Description and Method of Operation

Although this report is concerned with the aerodynamic design of the tunnel, some description of the wind tunnel and its operation will be given here. (See reference (1) for further details) Figure 5

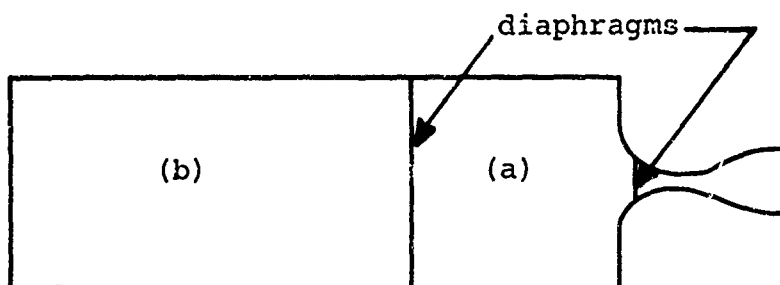
shows the layout and major components of the facility. The tunnel will have three legs, one for each Mach number, connected to a common bank of gas driver vessels and a vacuum sphere. The main elements in each leg will be a gas heater, nozzle, test cell, and diffuser. For reasons of economy, the test cell with the model support system will be mounted on a moveable transfer cart and will be used for all three tunnel legs.

The method of operation will be the same for each leg and is as follows. The three gas driver vessels, with a combined volume of 150 ft³, will be pressurized by mechanical compressors to a maximum of 40,000 psi (2720 atm). If necessary, heater elements in the driver vessels can then be used to raise the gas temperature to 290°F, creating a maximum pressure of 60,000 psi (4080 atm). At the same time, the nitrogen in the gas heater to be used is brought to the desired supply pressure and temperature by pumping and heating. The gas heater is separated from the nozzle by a series of diaphragms, which allows the nozzle, test section, diffuser, and vacuum sphere to be pre-evacuated. When the desired conditions have been obtained in all parts of the system, tunnel operation is initiated by rupturing the diaphragms and opening the pressure control valves between driver vessels and heater. The control valves are opened in such a way as to keep the gas heater pressure (the nozzle supply pressure) constant during the test run. The test run is terminated when all the hot gas from the heater has been expanded through the nozzle. The control valves are then closed, the diaphragms are replaced, and the cycle is repeated.

Pressure and Temperature Changes in the Heater Vessel

As mentioned in the preceding section, pressure control valves to be installed between the gas driver and heater vessels will open at a rate such as to maintain a constant pressure in the heater during the test run. However, it is likely that these valves will not be in place during the initial phases of the shakedown. Hence, it is worthwhile to consider pressure and temperature changes which may occur when the valves are of a simple open-closed type. With such valves the nozzle supply pressure and temperature will decrease during the run. This occurs because the pressure in the heater will fall due to

the mass outflow through the nozzle, and the temperature will also fall since the process may be considered isentropic. In order to illustrate this we will solve the following simple problem. The results should be reasonably close to those that occur in the actual process in the NOL Hypervelocity Wind Tunnel.



Imagine a non-heat-conducting diaphragm separating a cold gas identified by subscript (b) from a hot gas identified by subscript (a). Another diaphragm prevents the hot gas from escaping through the nozzle. The pressure in the two gases is equal. The two diaphragms are instantaneously removed. The actual flow process which ensues is a complex one of rarefaction and compression waves. However, one can calculate effective supply pressures and temperatures for the nozzle by making reasonable assumptions as follows.

(1) The nozzle throat opening is sufficiently small that the Mach number in the vessel is very low.

(2) The two gases do not mix and no heat is conducted between them.

(3) Stratification of the two gases in the neighborhood of the interface can be neglected. That is, we neglect the fact that the cold gas tends to flow under and ahead of the hot gas. A crude analysis shows that the parameter $\frac{t}{L} \sqrt{2gh(1 - \frac{\rho_a}{\rho_b})}$ should be kept small. L is the length of the hot region, t is the flow time, and h is the height of the heater. Experiments are required to determine how small the above parameter must be.

(4) Pressure losses due to friction and heat losses to the walls are negligible.

(5) The time scale of interest (τ) is considerably longer than the time scale for pressure adjustments in the vessel. We require

$$\tau \gg \frac{L}{a_b}$$

where L is the vessel length and a_b is the speed of sound in the cold gas

(6) The pressure in the vessel is constant at any particular time.

It is believed that all assumptions with the possible exception of (2) and (3) are well satisfied in the real process. The amount of mixing will depend on the mechanical arrangement but can probably be kept small. It is presently believed that stratification will not be a serious problem at Mach number 10. The Mach number 15 and 20 heaters will be installed vertically in order to avoid any stratification problem.

The above assumptions result in the following set of differential equations.

$$\frac{dp}{p} = \gamma_{E,a} \cdot \frac{d\rho_a}{\rho_a} \quad (1)$$

$$\frac{dm_a}{m_a} = \frac{d\rho_a}{\rho_a} + \frac{dV_a}{V_a} \quad (2)$$

$$\frac{dp}{p} = \gamma_{E,b} \frac{d\rho_b}{\rho_b} \quad (3)$$

$$dV_a + dV_b = 0 \quad (4)$$

$$\frac{d\rho_b}{\rho_b} + \frac{dV_b}{V_b} = 0 \quad (5)$$

The isentropic exponent γ_E in the above equations is given by

$$\gamma_E = \left. \frac{\rho}{p} \cdot \frac{dp}{d\rho} \right|_s = \frac{\rho a^2}{p} \quad (6)$$

Note that gas (a) only refers to the hot gas which remains in the vessel. Equations (1) and (3) state that thermodynamic changes in the vessel are isentropic. Equations (2), (4), and (5) arise from the definition of the mass m_a , the constancy of the total volume of the vessel, and constancy of the mass of gas (b), respectively. We regard equations (1) through (5) as five equations for the five unknowns - dp , $d\rho_a$, $d\rho_b$, dV_a , dV_b - in terms of dm_a .

We find

$$\frac{dp}{p} = \frac{dm_a}{\rho_a} \cdot \frac{1}{\left(\frac{V_a}{\gamma_{E,a}} + \frac{V_b}{\gamma_{E,b}} \right)} \quad (7)$$

and similar equations for the other four unknowns.

Let us now make use of the above relations to estimate the rate of pressure decay for the Hypervelocity Tunnel. We identify gas (b) with the cold storage gas, gas (a) with the gas in the heater and will assume that there is no pressure drop across the valve connecting the storage vessel and heater. One concludes from equation (7) that supply pressure changes may be decreased by

- (1) increasing the volume of heated gas
- (2) increasing the volume of cold gas
- (3) increasing the temperature at which the cold gas is stored since this decreases $\gamma_{E,b}$ (see Figure 6).

Let us now estimate the decrease in supply pressure which occurs when one expels all the hot gas from the heaters. We will use Figure 6 which shows γ_E as a function of pressure for various temperatures (data taken from reference (2)). Combine equations (3) and (5) to give

$$\frac{dp}{p} = - \gamma_{E,b} \frac{dV_b}{V_b} \quad (8)$$

That is, the fractional decrease in pressure is greater than the fractional increase in volume of the cold gas by the factor $\gamma_{E,b}$. Equation (8) will be used to estimate the pressure when the cold gas completely fills the heater volume. For the Mach number 15 and 20 heaters, equation (8) may be used in its differential form since the volume changes are relatively small. For the Mach 10 heater where dV_b is 0.37 of the initial cold gas volume, it is necessary to use equation (8) in its integrated form. Therefore, we will estimate the pressure changes for all Mach numbers by using an average (constant) value for $\gamma_{E,b}$ and integrate equation (8) to give

$$pV_b^{\gamma_{E,b}} = \text{constant} \quad (9)$$

We define $p_o^{(i)}$ to be the supply pressure at beginning of the run, $p_o^{(f)}$ to be the supply pressure at the time when the cold gas has completely filled the heater. The results are given in the following table.

| | Mach Number | | |
|--|-------------|------|------|
| | 10 | 15 | 20 |
| Heater volume (ft ³) | 45 | 9.6 | 6.3 |
| Running time (secs) | 1 | 1 | 5 |
| Storage volume (ft ³) | 122 | 122 | 122 |
| Temperature of stored gas (°K) | 400 | 400 | 400 |
| $\gamma_{E,b}$ | 2.1 | 4.5 | 4.8 |
| $p_o^{(i)}$ (atm) | 430 | 2365 | 3110 |
| $p_o^{(f)}$ (atm) | 222 | 1680 | 2440 |
| $\frac{p_o^{(i)} - p_o^{(f)}}{p_o^{(i)}} \times 100$ (%) | 48 | 29 | 21 |

The above table shows that appreciable supply pressure changes will occur for the Mach number 10 and 15 cases unless there is a control valve between the stored gas and the hot gas. In the Mach number 20 case, the change is much smaller, about 4 percent per second. It is desirable to provide some type of pressure control by starting the run with a pressure in the cold gas higher than that in the hot gas and programming the opening rate of the valve between the two vessels. The valve opening rate will not be considered further here because any analysis would depend on having more mechanical details of the valve than are presently available.

Let us now turn our attention to variations in supply temperature which accompany the variations in supply pressure. The two quantities vary together because, at least for our simplified model, the specific entropy of the gas in the heater remains constant. We have, omitting subscript (a),

$$\left. \frac{dT/T}{dp/p} \right|_s = \frac{p}{T} \cdot \left. \frac{dT}{dp} \right|_s \quad (10)$$

$$\begin{aligned} \text{Now } Tds &= dH - \frac{dp}{\rho} \\ &= C_p dT + dp \left[\left. \frac{\partial H}{\partial p} \right|_T - \frac{1}{\rho} \right] \end{aligned} \quad (11)$$

$$\text{Therefore } \left. \frac{dT}{dp} \right|_s = \frac{\left. \frac{1}{\rho} - \frac{\partial H}{\partial p} \right|_T}{C_p} \quad (12)$$

Substitution of equation (12) into (10) and use of the equation of state $p = \rho ZRT$ (13)

$$\text{results in } \left. \frac{dT/T}{dp/p} \right|_s = \frac{ZR}{C_p} \left[1 - \rho \left. \frac{\partial H}{\partial p} \right|_T \right] = \frac{\gamma' - 1}{\gamma'} \quad (14)$$

The definition of γ' in equation (14) is made by analogy with a perfect gas. Figure 7 shows a graph of $(\frac{dT}{T})/(\frac{dp}{p})$ as a function of pressure and temperature derived from the tabulated results of reference (2). We see that we may expect temperature variations about one quarter the value of the pressure variations. This fact could lead to condensation in the test section if the test-section conditions were on the verge of condensation at the beginning of a run.

Pressure and Temperature Changes in the Vacuum Sphere

Each diffuser is attached directly to the 200,000 cubic foot vacuum sphere. Before each run the sphere will be evacuated to 10 mm pressure. We shall estimate the sphere pressure as a function of the mass of hot nitrogen which enters it on the basis of a quasi-steady calculation - that is, we assume that the gas mixing process in the sphere occurs in a time short compared to the time of interest for this calculation. This may not be strictly true, but the results should give reasonable values for the sphere pressure for purposes of determining whether the volume is large enough for the sphere to do its function, namely, keep the back pressure low enough.

- We define
- m_i = mass of gas originally in the sphere at 530°R and 10 mm pressure,
 - m_{TG} = mass of hot nitrogen test gas which enters the sphere at the tunnel stagnation enthalpy H_o ,
 - E = internal energy per unit mass,
 - E_i = internal energy per unit mass of gas originally in sphere,
 - Q = heat removed from the gas by means of a heat exchanger at entrance to sphere,
 - V = sphere volume
- Subscript o = supply conditions in heater.

The amount of energy which is carried into the sphere by a mass of test gas m_{TG} (if one assumes constant p_o) is

$$m_{TG}E_o + \frac{m_{TG}}{\rho_o} p_o - Q$$

The first term accounts for the internal energy which the gas has in the heater; the second term represents the work which the cold driver gas does on the hot gas in pushing it out of the heater; and the final term allows for the effect which heat removal has. The final internal energy E of the gas in the sphere may be found from energy conservation by adding the energy initially in the sphere and the energy carried into the sphere by the mass m_{TG} , i.e.

$$E (m_{TG} + m_i) = E_i m_i + m_{TG} E_o + \frac{m_{TG}}{\rho_o} p_o - Q \quad (15)$$

By using the definition of the stagnation enthalpy H_o

$$H_o = E_o + \frac{p_o}{\rho_o} \quad (16)$$

we obtain

$$E = \frac{E_i m_i + m_{TG} H_o - Q}{m_{TG} + m_i} \quad (17)$$

We also have

$$\rho = \frac{m_{TG} + m_i}{V} \quad (18)$$

Since it is not presently intended to cool the gas entering the sphere we set $Q = 0$.

Equations (17) and (18) along with the thermodynamic properties of nitrogen are sufficient to determine the pressure and temperature of the gas in the sphere after a mass m_{TG} of test gas with stagnation enthalpy H_o has entered from the diffuser. Figure 8 and 9 show the pressure and temperature, respectively, as a function of m_{TG} for three stagnation enthalpies. The enthalpies correspond to Mach number 10, 15, and 20 operation.

The table below shows, among other things, values of the ratio of test section Pitot pressure/sphere pressure after all the mass in the heater has been put in the sphere. The table has been constructed for the design conditions for the three Mach numbers. From the table, it

| | Mach Number | | |
|---------------------------------|-------------|--------|--------|
| | 10 | 15 | 20 |
| Supply pressure p_o (atm) | 430 | 2365 | 3110 |
| Supply enthalpy H_o (BTU/lbm) | 492.4 | 1016.1 | 1593.7 |
| Mass of test gas m_{TG} (lbm) | 340 | 180 | 140 |
| Pitot pressure (atm) | 1.45 | 1.30 | .315 |
| (lb/ft ²) | 3067 | 2744 | 666 |
| Sphere pressure (atm) | .130 | .133 | .154 |
| (lb/ft ²) | 275 | 282 | 325 |
| Pitot/Sphere pressure | 11.1 | 9.7 | 2.0 |
| Gas temperature in sphere (°R) | 1870 | 2740 | 3570 |

appears that the only condition for which there need be any concern that the flow will break down before the completion of the run is the Mach 20 case. Even there, a diffuser able to recover one-half the Pitot pressure will prevent breakdown, and it is believed that a recovery pressure higher than this can be achieved. This conclusion has been drawn on the basis of one set of supply conditions for each Mach number. The conclusion is also valid for operation at other than the design conditions because the Pitot pressure and sphere pressure will change with the supply pressure in approximately the same proportions.

Properties of High Density Nitrogen

Thermodynamic Properties

Figures 3 and 4 have shown that in order to achieve the desired range of free-stream Reynolds numbers in the tunnel test-section at reasonable mass flow rates, it is necessary to use nozzle supply pressures of several thousand atmospheres for operation at Mach numbers of 15 and 20. The corresponding densities are sufficiently high that compressibility corrections to the equation of state must include at least the first two virial coefficients. The densities upstream of the heater vessel (which serves as the nozzle supply chamber) are even higher so that it may be necessary to use more than two virial coefficients in the compressibility correction.

Thermodynamic data including such virial corrections are usually given in tabular form (e.g. references (2) - (6)) or in the graphical form of a Mollier diagram (e.g. reference (7)). These tabulations and diagrams were used to provide the properties of nitrogen at high densities required for calculations concerning tunnel components upstream of the nozzle. Since the properties from the various sources do not differ appreciably over most of the range of interest and since little experimental evidence exists for distinguishing among them, the choice of source for a given calculation was based upon convenience. Although the tabular and graphical forms mentioned above are very useful for calculations done by hand, they are not very well suited to computer applications such as the computation of nozzle contours.

The need for nitrogen properties at moderately high densities in a form suitable for computer applications was filled by adapting a versatile computer program developed by Dr. Harold W. Woolley (reference (8)). This program can compute the properties of arbitrary mixtures of various components* at moderately-high densities by treating the mixture as a Cragoe-type gas with

$$\frac{\ln Z}{\rho} = B' + C'\rho \quad (19)$$

Z is the compressibility of the gas and ρ the density. The coefficients B' and C' have been determined by fitting experimental data. Because of its form, this expression leads to nitrogen properties which agree quite well with published tabulations (see Figure 10) provided that the density is not too high. For the enthalpy and entropy required in the nozzle supply reservoir (i.e. the heater vessel), values of temperature, pressure, density, compressibility, and speed of sound obtained using Woolley's computer program deviated from values obtained from interpolations of Brahinsky's tabulations (reference (2)) by less than 0.4 percent, 1.2 percent, and 1.6 percent for the Mach number 10, 15, and 20 nozzles, respectively. Accordingly, the

*Subroutines for the six components, nitrogen, oxygen, argon, neon, carbon dioxide, water vapor, were included.

computer program was judged sufficiently accurate and was used to provide the nitrogen properties required for computing the nozzle contours. It must be kept in mind that the nozzle calculations are for moderately-high density conditions. For higher densities, such as in the gas supply vessels upstream of the heater, Woolley's program can be significantly in error and should not be used except with the utmost caution.

Condensation Line Properties

In order to attain the highest test-section Reynolds number for a given supply pressure and test-section Mach number, the test-section temperature should be as low as possible. To see this, we anticipate the results somewhat and assume that the temperature and pressure in the test section are such that the perfect gas law applies, the specific heats are constant, and the viscosity is a function of temperature only. Then, for a given pressure and test-section Mach number, the Reynolds number is proportional to about the -1.25 power of the test section temperature and, therefore, increases as the temperature decreases. This behavior can be seen in Figure 11 for three supply pressures and a Mach number of 20.

In practice, a lower limit exists for the test-section temperature for any given supply pressure because the gaseous nitrogen will condense into the liquid phase if cooled sufficiently. This lower limit is the temperature at which the nitrogen is on the verge of condensing, i.e. the condensation temperature. Operation at this limit then becomes "condensation threshold operation". Using the temperature-pressure relation for the onset of condensation given by Din (reference (3), p. 86)

$$\log_{10} p \text{ (mmHg)} = 6.49594 - \frac{255.821}{T \text{ (}^\circ\text{K)} - 6.6} \quad (20)$$

the Reynolds number per foot for condensation-threshold operation at Mach number 20 is shown as a function of test-section temperature in Figure 11, together with the curves for constant pressure operation. The figure shows, as expected, that the minimum supply pressure necessary to produce a given Reynolds number per foot in the test

section is the pressure corresponding to condensation threshold operation.

The expression given by Din for the onset of condensation applies only if the nitrogen does not become supersaturated. Daum (reference (9)) shows that a substantial amount of supersaturation can occur when a test gas is expanded rapidly to high velocity and low pressure. If the distance from the upstream end of the uniform flow region to the test section is sufficiently short, the test gas will still be in a supersaturated state when it reaches the test section. Applying the procedure outlined by Daum, it was estimated that there could be no supersaturation in the Mach number 10 and 15 nozzles and only a minimal amount in the Mach number 20 nozzle. Later calculations based on the final nozzle designs agreed with the early estimates.

Since little or no supersaturation is indicated, Din's expression was chosen to represent the temperature-pressure relation at condensation threshold. If a temperature is given, the corresponding pressure for condensation threshold operation is obtained from Din's expression. The remaining thermodynamic properties can then be found from a Mollier diagram, perfect gas relations, or a computer program such as the one obtained from Woolley. Woolley's program was used so that the condensation line properties would be consistent with the properties obtained by using Woolley's program to compute isentropic expansions from the selected nozzle supply conditions. The pressure, density, entropy, enthalpy, and sound speed for condensation threshold operation are shown in Figures 12-16 and listed in Table 1. The derived quantities of mass flow per unit area and Reynolds number per foot are shown in Figures 17 and 18.

Viscosity

The determination of the nozzle supply and test conditions required the use of the viscosity of nitrogen for the calculation of the Reynolds number at the test conditions. To obtain the required viscosities, the dilute gas relation given by Hirschfelder, Curtis and Bird (reference (10)) was used. For nitrogen, this relation can be written as

$$\mu = 7.0066 \times 10^{-7} \frac{\sqrt{T}}{\Omega(2,2)^*} \left(\frac{\text{lbm}}{\text{ftsec}} \right) \quad (21)$$

where T is in degrees Kelvin, and the collision integral $\Omega^{(2,2)*}$ is given by

$$\Omega^{(2,2)*} = \frac{1}{3} \left[6.771 - 6.38(T^* - .5) + 6.6(T^* - .5)^2 - 4(T^* - .5)^3 \right] \quad (22)$$

with $T^* = T/91.46$

This expression for $\Omega^{(2,2)*}$ represents a fit of the data tabulated by Hirschfelder, et al., for the Lennard-Jones (6-12) potential in the range 30-80°K. The viscosity calculated using equations 21 and 22 is shown in Figure 19 and listed in Table 1.

For the turbulent boundary layer calculations, the viscosity of nitrogen was needed at higher temperatures and pressures. The necessary viscosities were obtained from the results of Brebach and Thodos (reference (11)) who give a reduced state correlation for the viscosity of diatomic gases at atmospheric pressure and a density dependent correction to account for higher pressures. Since correlations are given only for the viscosity for nitrogen temperatures less than 126.2°K and greater than 441.7°K, the viscosity data in the intermediate range and the density dependent correction data had to be fitted with suitable expressions. The final expressions used are given below.

$$\frac{\mu}{\mu_{T_C}} = \begin{cases} T_R^{0.979} & T \leq 126.2^\circ\text{K} \\ \frac{1.7884T_R^{1.5}}{0.7884 + T_R} & 126.2 \leq T \leq 441.7^\circ\text{K} \\ 1.196T_R^{0.659} & T \geq 441.7^\circ\text{K} \end{cases} \quad (23)$$

$$\frac{\Delta\mu}{\mu_{T_C}} = \frac{1198\rho + 6410\rho^2}{\mu_{T_C}} \times 10^{-5} \quad .01 \leq \rho \leq .35 \text{ g/cm}^3 \quad (24)$$

where $\mu_{T_C} = 1.8066 \times 10^{-7} \text{ lbf sec/ft}^2$

$$T_R = T/126.2$$

with μ expressed in lb f sec/ft^2 , T in $^\circ\text{K}$, and ρ in g/cm^3 .

To ensure that the viscosity used in the boundary layer calculations was continuous, the viscosity at the lower temperatures was obtained from the Brebach-Thodos correlation rather than the dilute-gas relationship (equations 21 and 22). Thus, the Reynolds numbers near the nozzle exit used in the boundary layer calculations will be about 2 percent lower than those expected on the basis of Figure 18.

Nozzle Design

Nozzle Supply and Test Conditions

Given the conditions along Din's condensation line, the corresponding nozzle supply (heater vessel) conditions can be calculated using Woolley's computer program. First, for a particular condensation-line temperature, the supply enthalpy can be calculated from the desired Mach number and the condensation-line enthalpy and sound speed obtained either from Figures 15 and 16 or from Table 1. Since the expansion process in the nozzle is isentropic, the supply entropy is given by Figure 14 or Table 1. For each supply enthalpy-entropy pair, the remaining supply conditions can now be calculated using Woolley's computer program. The resulting supply pressure variations with condensation line temperature are shown in Figure 20 for selected Mach numbers between 10 and 20. Similarly, the required supply temperatures and densities are shown in Figures 21 and 22, respectively.

As was mentioned previously, the particular choice of nozzle supply and test conditions represents a compromise between a number of desirable but conflicting features. Consideration was given to such factors as test duration, Reynolds number capability, heater size and strength, nozzle size, pumping and vacuum requirements, and others, in order to find the optimum operating conditions which could be attained within the limitations of the allocated funds. Figures 2, 3, and 4, relating the supply pressure, Reynolds number, mass flow rate, volume flow rate in the supply vessel, and the nozzle core diameter, were made to simplify the search for the optimum operating conditions at Mach numbers 10, 15, and 20, respectively. Similar figures for these and other Mach numbers can be prepared from the data given in Figures 17, 18, 20, and 22.

The nozzle supply and test section conditions resulting from this compromise are listed in Table 2.

Inviscid Core

The thermodynamic properties of nitrogen required for calculating an isentropic expansion from the chosen supply conditions were obtained using Woolley's computer program (reference (8)). These properties were then used in a second computer program* to produce the tape input required for the Axisymmetric Core Program described in reference (12). The latter program applies the method of characteristics to compute the flow of a real gas in the supersonic portion of the inviscid core. For the present calculations, the Axisymmetric Core Program of reference (12) was modified to include a third type of centerline Mach number distribution. This allowed the radius of curvature at the nozzle throat to be decreased significantly, thereby decreasing the total heat transfer to the throat region.

The subsonic portion of the inviscid core was defined by using a fourth-order polynomial in x (axial distance) to represent the subsonic core radius. The five constants in the polynomial were determined by specifying the inlet length and the radius and slope at the upstream end of the inlet, then matching at the throat ($x=0$) the radius, slope, and curvature obtained from the characteristics calculation in the supersonic portion. The assumption of one-dimensional flow was then used to obtain the inlet flow variables required for the boundary layer calculations. The slight discontinuity in flow variables at the throat due to the use of a one-dimensional calculation in the subsonic region and a two-dimensional calculation in the supersonic region has only a negligibly small effect on the boundary layer growth in the throat region. Selected coordinates of the inviscid core contour for the three nozzles are included in Table 3. The coordinates for the Mach number 20 nozzle may be significantly in error because of the neglect of the transpiration or film cooling which may be needed to preserve the nozzle throat (see next section).

*The details of all aspects of the nozzle design are presented more fully in reference (13).

Boundary Layer

After the contour of the inviscid core has been determined, it must be corrected in order to account for the growth of the boundary layer on the nozzle wall. This correction was made by adding to the inviscid core contour the displacement thickness determined using the real gas turbulent boundary layer calculation method presented by Tetervin in reference (14). In addition to the integral momentum equation and an empirical skin friction law, Tetervin's method utilizes an integral moment of momentum equation to calculate the momentum thickness, skin friction, and a parameter which determines the shape of the velocity profile. From these quantities the required displacement and boundary layer thicknesses are obtained. Vector addition of the displacement thickness to the inviscid core contour then gives the contour of the nozzle wall.

A FORTRAN IV computer program developed to apply Tetervin's turbulent boundary layer method to the present nozzle design calculations is included in reference (13). The program as developed can be used for air or nitrogen and is compatible with the method of characteristics program of reference (12) which was used to compute the supersonic portion of the inviscid core contour. For convenience, the calculation of the subsonic portion of the inviscid core contour described in the preceding section was incorporated into the boundary layer program. The user has the option to omit the inlet core calculation and begin the boundary layer calculations at or downstream of the nozzle throat. Reference (13) includes full details of the program and directions for its use.

In the present calculations, the subsonic inviscid core option was utilized. Then the turbulent boundary layer growth was computed from the beginning of the subsonic inlet to the exit of the nozzle using the empirical Spalding-Chi skin friction law (reference (15)) and the Brebach-Thodos viscosity correlation for nitrogen discussed previously. Selected coordinates of the resulting nozzle contours are given in Table 3 together with the coordinates of the inviscid core contour.

The boundary layer calculations mentioned above assume that the nozzle wall temperature can be kept to a reasonable level without transpiration or film cooling. This can be done for the Mach number 10 nozzle and probably for the Mach number 15 nozzle. However, heat transfer calculations for the Mach number 20 nozzle show that massive transpiration or film cooling may be necessary in the throat region to keep the nozzle throat from failing early in the test run. Since the necessary designs and calculations have not been completed, nozzle coordinates obtained from preliminary calculations which did not take such cooling into account are presented in Table 3.

Nozzle Dimensions

In order to be able to use the same test cell and model support system for all three nozzles, the three nozzles were designed to have the same exit diameters and the same lengths. Preliminary calculations indicated that a throat-to-exit length of about 45 feet and an exit diameter of about 5 feet would be necessary for the Mach number 20 nozzle if the maximum expansion half-angle was to be kept near 12° . It was decided to design the nozzles such that at a distance of 40 feet from the nozzle throat the nozzle diameter would be five feet. The remaining portion of the nozzle would not be fabricated, since, if this cut-off portion was not too long, the nozzle performance would not be appreciably affected. The optimum cut-off point is that axial location at which the boundary layer enters the uniform flow region inside the Mach cone (see Figure 23). Downstream of this point, the usable test core decreases, even though the cross-sectional area of the nozzle continues to increase. Iterations involving the boundary layer program only, were sufficient to produce contours for the Mach number 10 and 15 nozzles in which the optimum cut-off point occurred within a few inches of the 40-foot station. These small differences made further iterations unnecessary and the nozzles were cut-off at the 40-foot station. The length of the cut-off portion was 1.72 and 1.50 feet for the Mach number 10 and 15 nozzles, respectively. For the Mach number 20 nozzle, the optimum cut-off point occurred at the 44.7-foot station or 1.88 feet from the end of the uncut nozzle. To move the optimum cut-off point nearer to the

40-foot station would require a maximum expansion angle appreciably greater than any considered acceptable. For this reason, no further iterations were made for the Mach number 20 nozzle. The diameter of the usable test core was 18.2 inches at the 40 foot cut-off point rather than the 21 inches which would have been attained if the nozzle had been cut-off at the optimum location. The seven square foot test core thus obtained was considered adequate. Principal dimensions of the three nozzles are given in Table 4.

Concluding Remarks

The NOL Hypervelocity Wind Tunnel is a unique aerodynamic facility for hypersonic research and developmental testing. The capability of achieving a high Mach number - high Reynolds number flow with relatively long run times and large model sizes will permit the accumulation of large amounts of aerodynamic test data, greatly facilitating the design and development of advanced, high-performance re-entry vehicles.

This report summarizing the aerodynamic design of the facility is the first of a series. Other technical reports documenting various aspects of the aerodynamic and mechanical design, tunnel performance, and test results obtained will be published as the material becomes available.

References

1. Glowacki, W.J., Harris, E.L., Lobb, R.K., and Schlesinger, M.I., "The NOL Hypervelocity Wind Tunnel," AIAA Preprint 71-253, Albuquerque, N.M., March 1971
2. Brahinsky, H.S., and Neel, C.A., "Tables of Equilibrium Thermodynamic Properties of Nitrogen," AEDC-TR-69-126, Aug 1969
3. Din, F., Thermodynamic Functions of Gases, Vol. 3, Methane, Nitrogen, Ethane, Butterworths, London, 1961
4. Hilsenrath, J., and Klein, M., "Tables of Thermodynamic Properties of Nitrogen in Chemical Equilibrium including Second Virial Corrections from 2000°K to 15,000°K," AEDC-TDR-63-162, Mar 1964
5. Smith, C.E., Jr., "Thermodynamic Properties of Nitrogen," LMSC L-90-62-111, Dec 1962
6. Grabau, M., and Brahinsky, H.S., "Thermodynamic Properties of Nitrogen from 300 to 5000°K and from 1 to 1000 Amagats," AEDC-TR-66-69, Aug 1966
7. Humphrey, R.L. and Piper, C.H., "Mollier Diagram for Nitrogen," NOLTR 67-32, 14 Mar 1967
8. Woolley, H.S., National Bureau of Standards, Gaithersburg, MD, private communication
9. Daum, F.L. and Gyarmathy, G., "Condensation of Air and Nitrogen in Hypersonic Wind Tunnels," AIAA Journal, Vol. 6, No. 3, p. 458, Mar 1968
10. Hirschfelder, J.O., Curtiss, C.F., and Bird, R.B., Molecular Theory of Gases and Liquids, John Wiley and Sons, New York, 1954
11. Brebach, W.J. and Thodos, G., "Viscosity - Reduced State Correlation for Diatomic Gases," Ind. Eng. Chem., Vol. 50, No. 7, p. 1095, July 1958
12. Glowacki, W.J., "FORTRAN IV (IBM 7090) Program for the Design of Contoured Axisymmetric Nozzles for High Temperature Air," NOLTR 64-219, Feb 1965
13. Glowacki, W.J., "NOL Hypervelocity Wind Tunnel, Report No. 2: Nozzle Design," NOLTR 71-6, Apr 1971

NOLTR 71-5

14. Tetervin, N., "NOL Hypervelocity Wind Tunnel, Report No. 3: Theoretical Analysis of the Boundary Layer in the Nozzles," NOLTR 71-7, Feb 1971
15. Spalding, D.B. and Chi, S.W., "The Drag of a Compressible Turbulent Boundary Layer on a Smooth Flat Plate With and Without Heat Transfer," J. Fluid Mech. Vol. 18, pp 117-143, 1964

NOLTR 71-5

TABLE 1
NITROGEN PROPERTIES AT CONDENSATION THRESHOLD

| TEMPERATURE °K | PRESSURE ATM | DENSITY AMAGAT | ENTROPY* | ENTHALPY BTU/LBM | SOUND SPEED FT/SEC | VISCOSITY LBM/FT SEC |
|-------------------|-----------------|-------------------|----------|---------------------|--------------------------|-------------------------|
| 40.0 | 9.0327E-05 | 6.1656E-04 | 25.312 | 17.755 | 422.96 | 1.8470E-06 |
| 40.2 | 1.0033E-04 | 6.8140E-04 | 25.225 | 17.845 | 424.01 | 1.8557E-06 |
| 40.4 | 1.1129E-04 | 7.5214E-04 | 25.139 | 17.934 | 425.07 | 1.8644E-06 |
| 40.6 | 1.2331E-04 | 8.2923E-04 | 25.053 | 18.023 | 426.12 | 1.8731E-06 |
| 40.8 | 1.3645E-04 | 9.1315E-04 | 24.969 | 18.113 | 427.16 | 1.8818E-06 |
| 41.0 | 1.5082E-04 | 1.0044E-03 | 24.886 | 18.202 | 428.21 | 1.8906E-06 |
| 41.2 | 1.6652E-04 | 1.1035E-03 | 24.804 | 18.292 | 429.25 | 1.8993E-06 |
| 41.4 | 1.8363E-04 | 1.2111E-03 | 24.723 | 18.381 | 430.29 | 1.9080E-06 |
| 41.6 | 2.0228E-04 | 1.3277E-03 | 24.643 | 18.470 | 431.33 | 1.9168E-06 |
| 41.8 | 2.2258E-04 | 1.4539E-03 | 24.565 | 18.560 | 432.36 | 1.9256E-06 |
| 42.0 | 2.4465E-04 | 1.5905E-03 | 24.487 | 18.649 | 433.39 | 1.9343E-06 |
| 42.2 | 2.6862E-04 | 1.7380E-03 | 24.410 | 18.738 | 434.42 | 1.9431E-06 |
| 42.4 | 2.9464E-04 | 1.8974E-03 | 24.334 | 18.828 | 435.45 | 1.9519E-06 |
| 42.6 | 3.2284E-04 | 2.0693E-03 | 24.259 | 18.917 | 436.48 | 1.9607E-06 |
| 42.8 | 3.5339E-04 | 2.2545E-03 | 24.185 | 19.006 | 437.50 | 1.9695E-06 |
| 43.0 | 3.8644E-04 | 2.4539E-03 | 24.112 | 19.095 | 438.52 | 1.9783E-06 |
| 43.2 | 4.2217E-04 | 2.6683E-03 | 24.040 | 19.185 | 439.53 | 1.9871E-06 |
| 43.4 | 4.6076E-04 | 2.8988E-03 | 23.968 | 19.274 | 440.55 | 1.9959E-06 |
| 43.6 | 5.0240E-04 | 3.1463E-03 | 23.898 | 19.363 | 441.56 | 2.0048E-06 |
| 43.8 | 5.4729E-04 | 3.4119E-03 | 23.828 | 19.453 | 442.57 | 2.0136E-06 |
| 44.0 | 5.9566E-04 | 3.6965E-03 | 23.760 | 19.542 | 443.58 | 2.0225E-06 |
| 44.2 | 6.4771E-04 | 4.0014E-03 | 23.692 | 19.631 | 444.58 | 2.0313E-06 |
| 44.4 | 7.0368E-04 | 4.3277E-03 | 23.625 | 19.720 | 445.59 | 2.0402E-06 |
| 44.6 | 7.6383E-04 | 4.6765E-03 | 23.558 | 19.810 | 446.59 | 2.0490E-06 |
| 44.8 | 8.2841E-04 | 5.0493E-03 | 23.493 | 19.899 | 447.58 | 2.0579E-06 |
| 45.0 | 8.9769E-04 | 5.4473E-03 | 23.428 | 19.988 | 448.58 | 2.0668E-06 |
| 45.2 | 9.7195E-04 | 5.8719E-03 | 23.364 | 20.077 | 449.57 | 2.0757E-06 |
| 45.4 | 1.0515E-03 | 6.3245E-03 | 23.301 | 20.166 | 450.56 | 2.0846E-06 |
| 45.6 | 1.1366E-03 | 6.8067E-03 | 23.238 | 20.256 | 451.55 | 2.0935E-06 |
| 45.8 | 1.2277E-03 | 7.3199E-03 | 23.177 | 20.345 | 452.54 | 2.1024E-06 |
| 46.0 | 1.3250E-03 | 7.8659E-03 | 23.116 | 20.434 | 453.52 | 2.1114E-06 |
| 46.2 | 1.4289E-03 | 8.4462E-03 | 23.055 | 20.523 | 454.50 | 2.1203E-06 |
| 46.4 | 1.5398E-03 | 9.0626E-03 | 22.996 | 20.612 | 455.48 | 2.1292E-06 |
| 46.6 | 1.6581E-03 | 9.7170E-03 | 22.937 | 20.701 | 456.46 | 2.1382E-06 |
| 46.8 | 1.7841E-03 | 1.0411E-02 | 22.878 | 20.791 | 457.43 | 2.1471E-06 |
| 47.0 | 1.9183E-03 | 1.1147E-02 | 22.821 | 20.880 | 458.40 | 2.1561E-06 |
| 47.2 | 2.0612E-03 | 1.1926E-02 | 22.764 | 20.969 | 459.37 | 2.1650E-06 |
| 47.4 | 2.2131E-03 | 1.2752E-02 | 22.707 | 21.058 | 460.34 | 2.1740E-06 |
| 47.6 | 2.3746E-03 | 1.3625E-02 | 22.652 | 21.147 | 461.30 | 2.1830E-06 |
| 47.8 | 2.5461E-03 | 1.4548E-02 | 22.596 | 21.236 | 462.27 | 2.1920E-06 |
| 48.0 | 2.7282E-03 | 1.5524E-02 | 22.542 | 21.325 | 463.23 | 2.2010E-06 |
| 48.2 | 2.9214E-03 | 1.6555E-02 | 22.488 | 21.414 | 464.19 | 2.2099E-06 |
| 48.4 | 3.1262E-03 | 1.7642E-02 | 22.435 | 21.503 | 465.14 | 2.2190E-06 |
| 48.6 | 3.3431E-03 | 1.8789E-02 | 22.382 | 21.592 | 466.09 | 2.2280E-06 |
| 48.8 | 3.5729E-03 | 1.9999E-02 | 22.330 | 21.681 | 467.05 | 2.2370E-06 |
| 49.0 | 3.8161E-03 | 2.1274E-02 | 22.278 | 21.770 | 467.99 | 2.2460E-06 |
| 49.2 | 4.0733E-03 | 2.2616E-02 | 22.227 | 21.858 | 468.94 | 2.2550E-06 |
| 49.4 | 4.3451E-03 | 2.4028E-02 | 22.177 | 21.947 | 469.88 | 2.2641E-06 |
| 49.6 | 4.6324E-03 | 2.5514E-02 | 22.127 | 22.036 | 470.83 | 2.2731E-06 |
| 49.8 | 4.9357E-03 | 2.7076E-02 | 22.078 | 22.125 | 471.77 | 2.2821E-06 |

* ENTROPY S EXPRESSED IN DIMENSIONLESS FORM S/R

NOLTR 71-5

TABLE 1 (CONT.)

| TEMPERATURE °K | PRESSURE ATM | DENSITY AMAGAT | ENTROPY* | ENTHALPY BTU/LBM | SOUND SPEED FT/SEC | VISCOSITY LBM/FT SEC |
|-------------------|-----------------|-------------------|----------|---------------------|--------------------------|-------------------------|
| 50.0 | 5.2558E-03 | 2.8718E-02 | 22.029 | 22.214 | 472.70 | 2.2912E-06 |
| 50.2 | 5.5934E-03 | 3.0442E-02 | 21.980 | 22.302 | 473.64 | 2.3003E-06 |
| 50.4 | 5.9493E-03 | 3.2252E-02 | 21.933 | 22.391 | 474.57 | 2.3093E-06 |
| 50.6 | 6.3244E-03 | 3.4150E-02 | 21.885 | 22.480 | 475.50 | 2.3184E-06 |
| 50.8 | 6.7193E-03 | 3.6142E-02 | 21.838 | 22.568 | 476.43 | 2.3275E-06 |
| 51.0 | 7.1350E-03 | 3.8229E-02 | 21.792 | 22.657 | 477.36 | 2.3365E-06 |
| 51.2 | 7.5724E-03 | 4.0415E-02 | 21.746 | 22.746 | 478.28 | 2.3456E-06 |
| 51.4 | 8.0323E-03 | 4.2705E-02 | 21.701 | 22.834 | 479.20 | 2.3547E-06 |
| 51.6 | 8.5157E-03 | 4.5101E-02 | 21.656 | 22.923 | 480.12 | 2.3638E-06 |
| 51.8 | 9.0235E-03 | 4.7608E-02 | 21.611 | 23.011 | 481.03 | 2.3729E-06 |
| 52.0 | 9.5567E-03 | 5.0230E-02 | 21.567 | 23.100 | 481.95 | 2.3820E-06 |
| 52.2 | 1.0116E-02 | 5.2970E-02 | 21.524 | 23.188 | 482.86 | 2.3911E-06 |
| 52.4 | 1.0703E-02 | 5.5833E-02 | 21.481 | 23.276 | 483.77 | 2.4002E-06 |
| 52.6 | 1.1319E-02 | 5.8823E-02 | 21.438 | 23.365 | 484.68 | 2.4094E-06 |
| 52.8 | 1.1964E-02 | 6.1943E-02 | 21.396 | 23.453 | 485.58 | 2.4185E-06 |
| 53.0 | 1.2640E-02 | 6.5199E-02 | 21.354 | 23.541 | 486.48 | 2.4276E-06 |
| 53.2 | 1.3348E-02 | 6.8596E-02 | 21.313 | 23.629 | 487.38 | 2.4368E-06 |
| 53.4 | 1.4099E-02 | 7.2136E-02 | 21.272 | 23.717 | 488.28 | 2.4459E-06 |
| 53.6 | 1.4864E-02 | 7.5826E-02 | 21.231 | 23.806 | 489.18 | 2.4550E-06 |
| 53.8 | 1.5674E-02 | 7.9664E-02 | 21.191 | 23.894 | 490.07 | 2.4642E-06 |
| 54.0 | 1.6522E-02 | 8.3672E-02 | 21.151 | 23.982 | 490.96 | 2.4733E-06 |
| 54.2 | 1.7408E-02 | 8.7838E-02 | 21.112 | 24.070 | 491.85 | 2.4825E-06 |
| 54.4 | 1.8333E-02 | 9.2172E-02 | 21.073 | 24.157 | 492.73 | 2.4917E-06 |
| 54.6 | 1.9299E-02 | 9.6680E-02 | 21.034 | 24.245 | 493.62 | 2.5008E-06 |
| 54.8 | 2.0307E-02 | 1.0137E-01 | 20.996 | 24.333 | 494.50 | 2.5100E-06 |
| 55.0 | 2.1359E-02 | 1.0624E-01 | 20.958 | 24.421 | 495.38 | 2.5192E-06 |
| 55.2 | 2.2456E-02 | 1.1130E-01 | 20.920 | 24.508 | 496.25 | 2.5284E-06 |
| 55.4 | 2.3599E-02 | 1.1655E-01 | 20.883 | 24.596 | 497.13 | 2.5376E-06 |
| 55.6 | 2.4791E-02 | 1.2201E-01 | 20.846 | 24.684 | 498.00 | 2.5467E-06 |
| 55.8 | 2.6033E-02 | 1.2767E-01 | 20.810 | 24.771 | 498.86 | 2.5559E-06 |
| 56.0 | 2.7325E-02 | 1.3355E-01 | 20.774 | 24.858 | 499.73 | 2.5651E-06 |
| 56.2 | 2.8671E-02 | 1.3964E-01 | 20.738 | 24.946 | 500.59 | 2.5743E-06 |
| 56.4 | 3.0072E-02 | 1.4596E-01 | 20.702 | 25.033 | 501.46 | 2.5835E-06 |
| 56.6 | 3.1529E-02 | 1.5250E-01 | 20.667 | 25.120 | 502.31 | 2.5927E-06 |
| 56.8 | 3.3044E-02 | 1.5929E-01 | 20.633 | 25.207 | 503.17 | 2.6020E-06 |
| 57.0 | 3.4619E-02 | 1.6631E-01 | 20.598 | 25.294 | 504.02 | 2.6112E-06 |
| 57.2 | 3.6256E-02 | 1.7358E-01 | 20.564 | 25.381 | 504.87 | 2.6204E-06 |
| 57.4 | 3.7956E-02 | 1.8111E-01 | 20.530 | 25.468 | 505.72 | 2.6296E-06 |
| 57.6 | 3.9722E-02 | 1.8890E-01 | 20.497 | 25.555 | 506.57 | 2.6388E-06 |
| 57.8 | 4.1555E-02 | 1.9696E-01 | 20.464 | 25.642 | 507.41 | 2.6481E-06 |
| 58.0 | 4.3458E-02 | 2.0529E-01 | 20.431 | 25.729 | 508.25 | 2.6573E-06 |
| 58.2 | 4.5432E-02 | 2.1390E-01 | 20.398 | 25.815 | 509.09 | 2.6666E-06 |
| 58.4 | 4.7479E-02 | 2.2280E-01 | 20.366 | 25.902 | 509.92 | 2.6758E-06 |
| 58.6 | 4.9602E-02 | 2.3200E-01 | 20.334 | 25.988 | 510.76 | 2.6850E-06 |
| 58.8 | 5.1802E-02 | 2.4150E-01 | 20.302 | 26.075 | 511.59 | 2.6943E-06 |
| 59.0 | 5.4082E-02 | 2.5131E-01 | 20.271 | 26.161 | 512.42 | 2.7035E-06 |
| 59.2 | 5.6443E-02 | 2.6144E-01 | 20.239 | 26.247 | 513.24 | 2.7128E-06 |
| 59.4 | 5.8889E-02 | 2.7188E-01 | 20.209 | 26.333 | 514.06 | 2.7220E-06 |
| 59.6 | 6.1421E-02 | 2.8266E-01 | 20.178 | 26.419 | 514.88 | 2.7313E-06 |
| 59.8 | 6.4042E-02 | 2.9379E-01 | 20.148 | 26.505 | 515.70 | 2.7406E-06 |

* ENTROPY IS EXPRESSED IN DIMENSIONLESS FORM S/R

NOLTR 71-5

TABLE 2

NOZZLE SUPPLY AND TEST SECTION CONDITIONS

| MACH NUMBER | 10 | 15 | 20 | |
|--|-------|-------|-------|---------------------|
| SUPPLY | | | | |
| PRESSURE | 430. | 2365. | 3110. | ATM |
| TEMPERATURE | 1854. | 3317. | 5040. | °R |
| ENTHALPY | 492.4 | 1016. | 1594. | BTU/LBM |
| DENSITY | 7.721 | 18.68 | 16.92 | LBM/FT ³ |
| TEST SECTION | | | | |
| PRESSURE X 10 ² | 1.127 | 0.448 | .0612 | ATM |
| TEMPERATURE | 94.64 | 89.10 | 79.31 | °R |
| DENSITY X 10 ³ | 4.567 | 1.929 | 0.296 | LBM/FT ³ |
| VELOCITY | 4846. | 7055. | 8877. | FT/SEC |
| REYNOLDS NUMBER PER FOOT X 10 ⁻⁶ | 9.2 | 6.0 | 1.3 | |

TABLE 3
 SELECTED INVISCID CORE AND NOZZLE WALL COORDINATES

| DISTANCE FROM THROAT (FT) | MACH NUMBER = 10 | | MACH NUMBER = 15 | | MACH NUMBER = 20 | |
|------------------------------------|---------------------------|---------------------------|---------------------------|---------------------------|---------------------------|---------------------------|
| | RADIUS OF CORE (FT) | RADIUS OF WALL (FT) | RADIUS OF CORE (FT) | RADIUS OF WALL (FT) | RADIUS OF CORE (FT) | RADIUS OF WALL (FT) |
| 0.0 | 0.09994 | 0.10014 | 0.03709 | 0.03715 | 0.01370 | 0.01373 |
| 0.1 | 0.10057 | 0.10085 | 0.04370 | 0.04387 | 0.02479 | 0.02503 |
| 0.2 | 0.10221 | 0.10258 | 0.05800 | 0.05839 | 0.04528 | 0.04606 |
| 0.3 | 0.10469 | 0.10516 | 0.07626 | 0.07699 | 0.06595 | 0.06755 |
| 0.5 | 0.11179 | 0.11246 | 0.11516 | 0.11688 | 0.10602 | 0.10996 |
| 1.0 | 0.13935 | 0.14077 | 0.21255 | 0.21823 | 0.20345 | 0.21538 |
| 1.5 | 0.17827 | 0.18087 | 0.30935 | 0.32039 | 0.29259 | 0.31209 |
| 2 | 0.22696 | 0.23127 | 0.40288 | 0.41882 | 0.37231 | 0.39949 |
| 3 | 0.34968 | 0.35921 | 0.56943 | 0.59509 | 0.51100 | 0.55394 |
| 4 | 0.49646 | 0.51339 | 0.71350 | 0.74908 | 0.62961 | 0.68870 |
| 5 | 0.65095 | 0.67609 | 0.84014 | 0.88592 | 0.73345 | 0.80905 |
| 6 | 0.80043 | 0.83370 | 0.95284 | 1.00911 | 0.82574 | 0.91821 |
| 8 | 1.06701 | 1.11619 | 1.14539 | 1.22353 | 0.98365 | 1.11091 |
| 10 | 1.28839 | 1.35378 | 1.30395 | 1.40520 | 1.11425 | 1.27777 |
| 12 | 1.47135 | 1.55363 | 1.43618 | 1.56172 | 1.22395 | 1.42510 |
| 15 | 1.68795 | 1.79674 | 1.59597 | 1.75977 | 1.35805 | 1.61776 |
| 20 | 1.93334 | 2.08844 | 1.78532 | 2.01621 | 1.52103 | 1.88212 |
| 25 | 2.07652 | 2.27842 | 1.90504 | 2.20446 | 1.62920 | 2.09307 |
| 30 | 2.15059 | 2.39696 | 1.97496 | 2.34140 | 1.69779 | 2.26223 |
| 35 | 2.17996 | 2.46516 | 2.00893 | 2.43784 | 1.73703 | 2.39652 |
| 40 | 2.18554 | 2.50000 | 2.01834 | 2.50000 | 1.75474 | 2.50000 |

NOLTR 71-5

TABLE 4
SELECTED NOZZLE DIMENSIONS

| MACH NUMBER | 10 | 15 | 20 |
|-------------------------|--------|--------|--------|
| LENGTH (FT) | | | |
| INLET | 0.75 | 0.45 | 0.40 |
| EXPANSION | 40.00 | 40.00 | 40.00 |
| TOTAL | 40.75 | 40.45 | 40.40 |
| DIAMETER (FT) | | | |
| ENTRANCE | 0.679 | 0.383 | 0.333 |
| THROAT | 0.200 | 0.074 | 0.028 |
| EXIT | 5.000 | 5.000 | 5.000 |
| CORE* | 4.371 | 4.037 | 3.509 |
| USABLE** | 4.005 | 3.752 | 3.282 |
| AREA (FT ²) | | | |
| ENTRANCE | 0.3622 | 0.1154 | 0.0872 |
| THROAT | 0.0315 | 0.0043 | 0.0006 |
| EXIT | 19.635 | 19.635 | 19.635 |
| CORE* | 15.006 | 12.798 | 9.6729 |
| USABLE** | 12.596 | 11.059 | 8.4588 |

* INVISCID CORE MEASURED AT NOZZLE EXIT

** USABLE DIAMETER AT NOZZLE EXIT DEFINED AS THE NOZZLE EXIT DIAMETER MINUS TWICE THE BOUNDARY LAYER THICKNESS AT THE EXIT

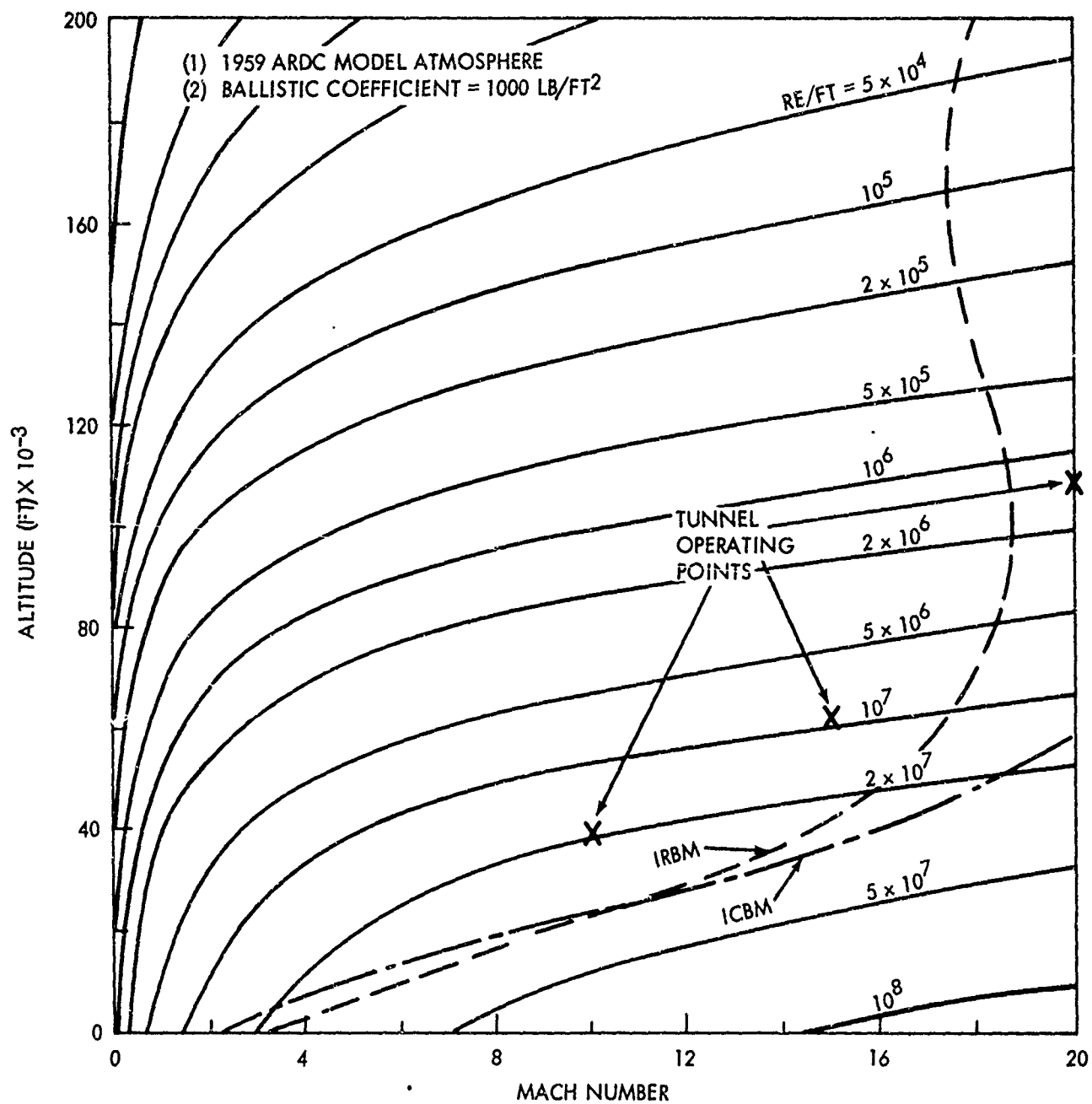


FIGURE 1 COMPARISON OF FREE-FLIGHT REYNOLDS NUMBERS WITH THOSE AVAILABLE IN THE FACILITY

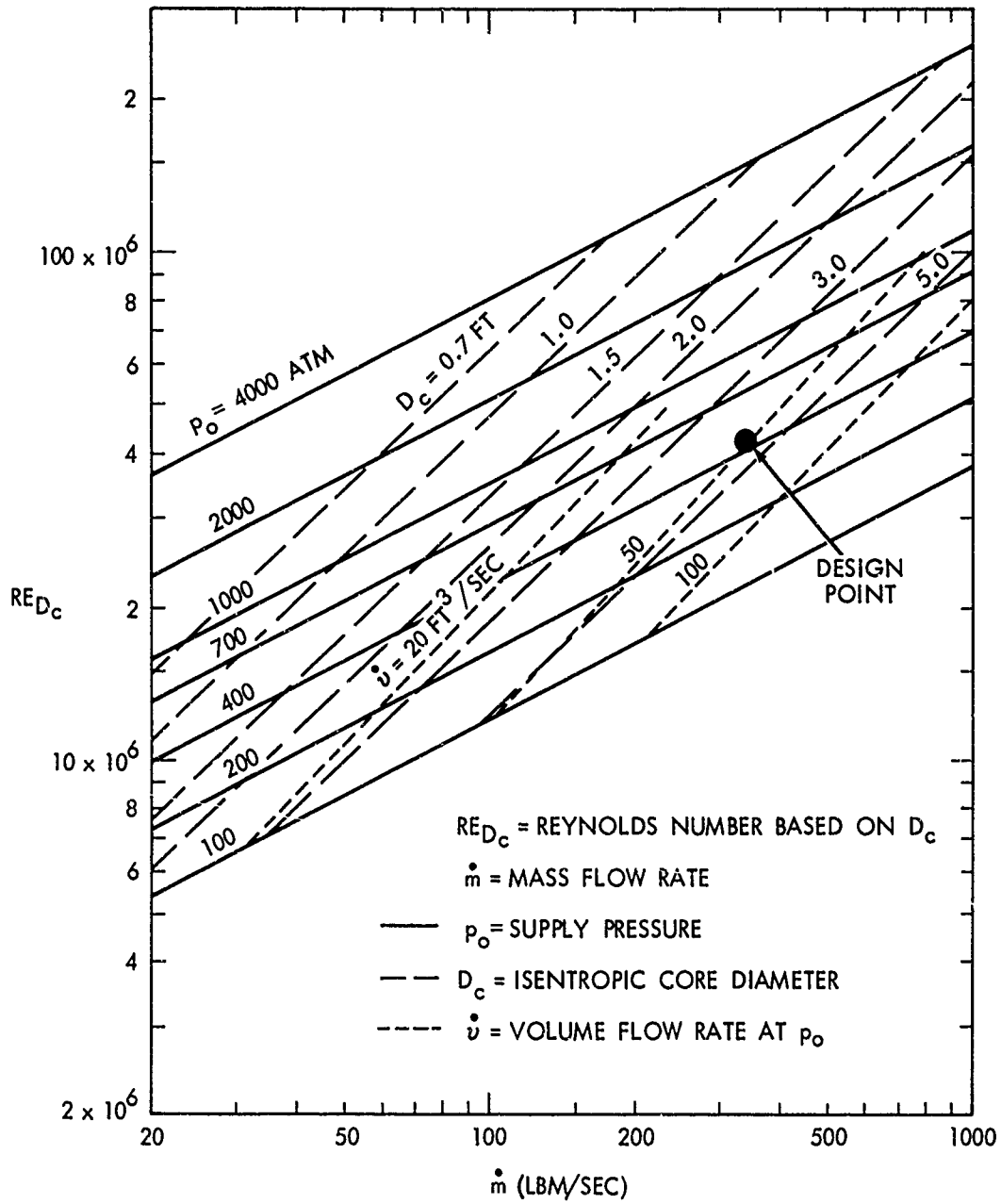


FIGURE 2 REQUIRED SUPPLY PRESSURE, CORE DIAMETER, AND VOLUME FLOW RATE FOR GIVEN RE_{D_c} AND MASS FLOW RATE (MACH 10)

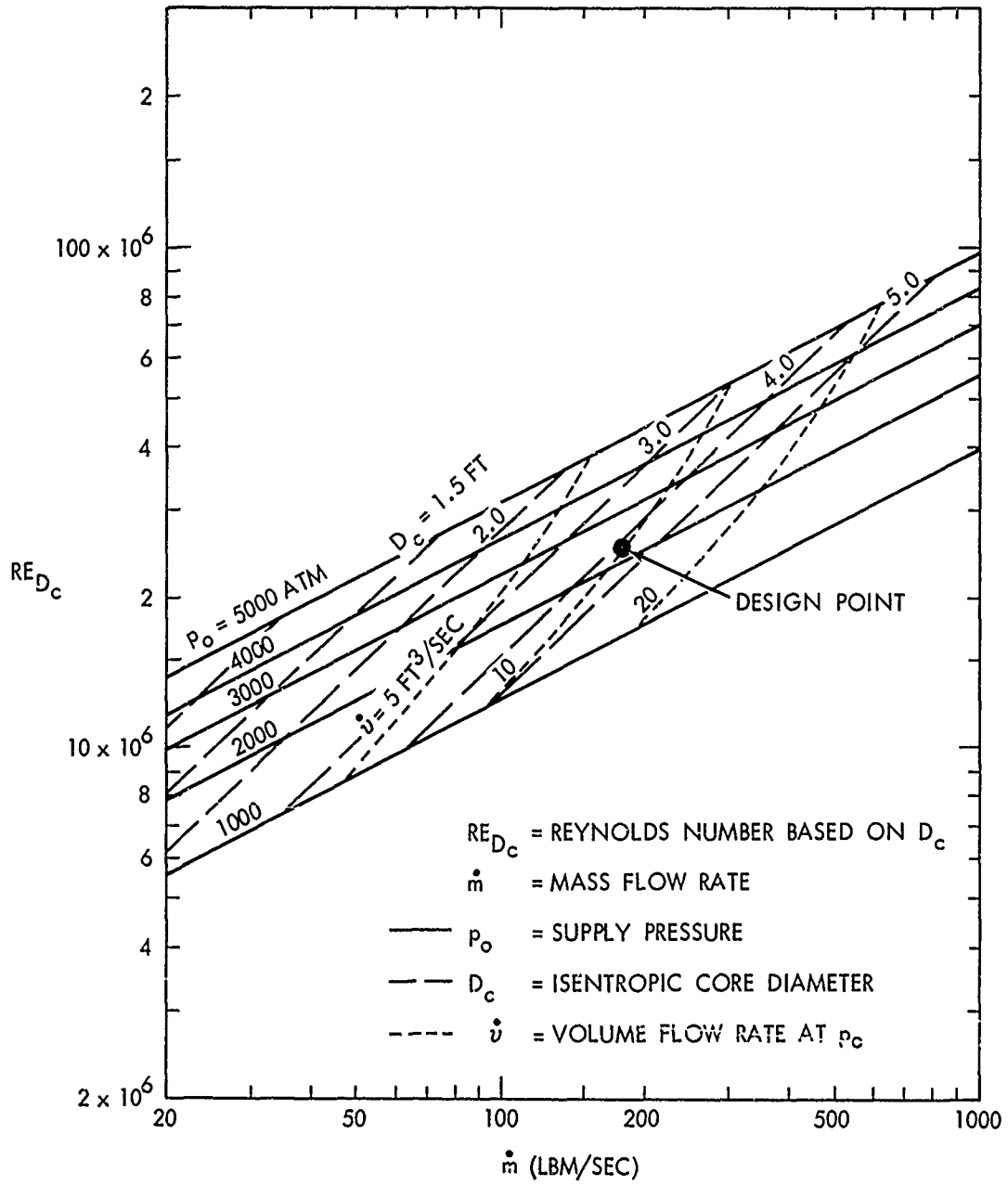


FIGURE 3 REQUIRED SUPPLY PRESSURE, CORE DIAMETER, AND VOLUME FLOW RATE FOR GIVEN RE_{D_c} AND MASS FLOW RATE (MACH 15)

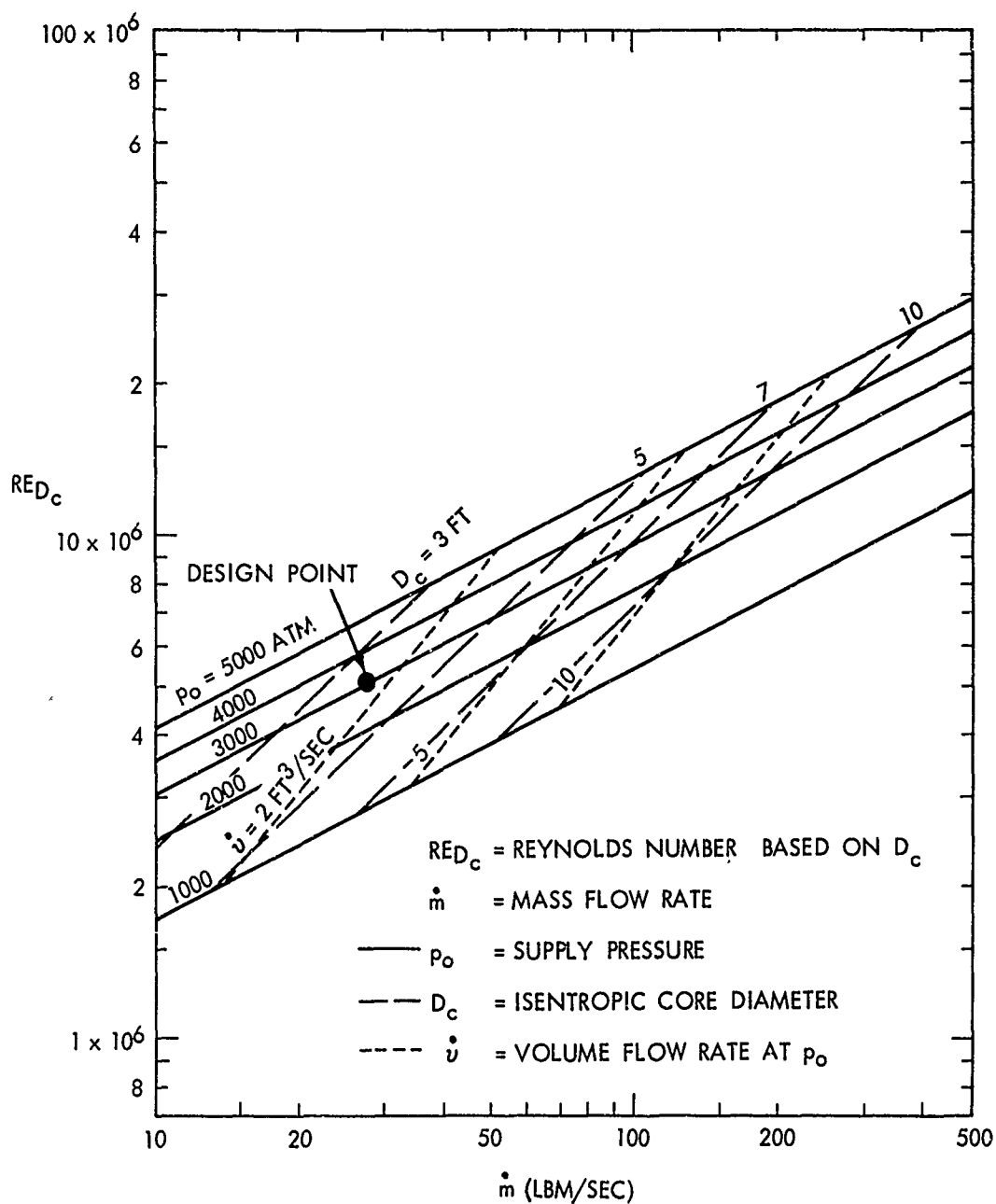
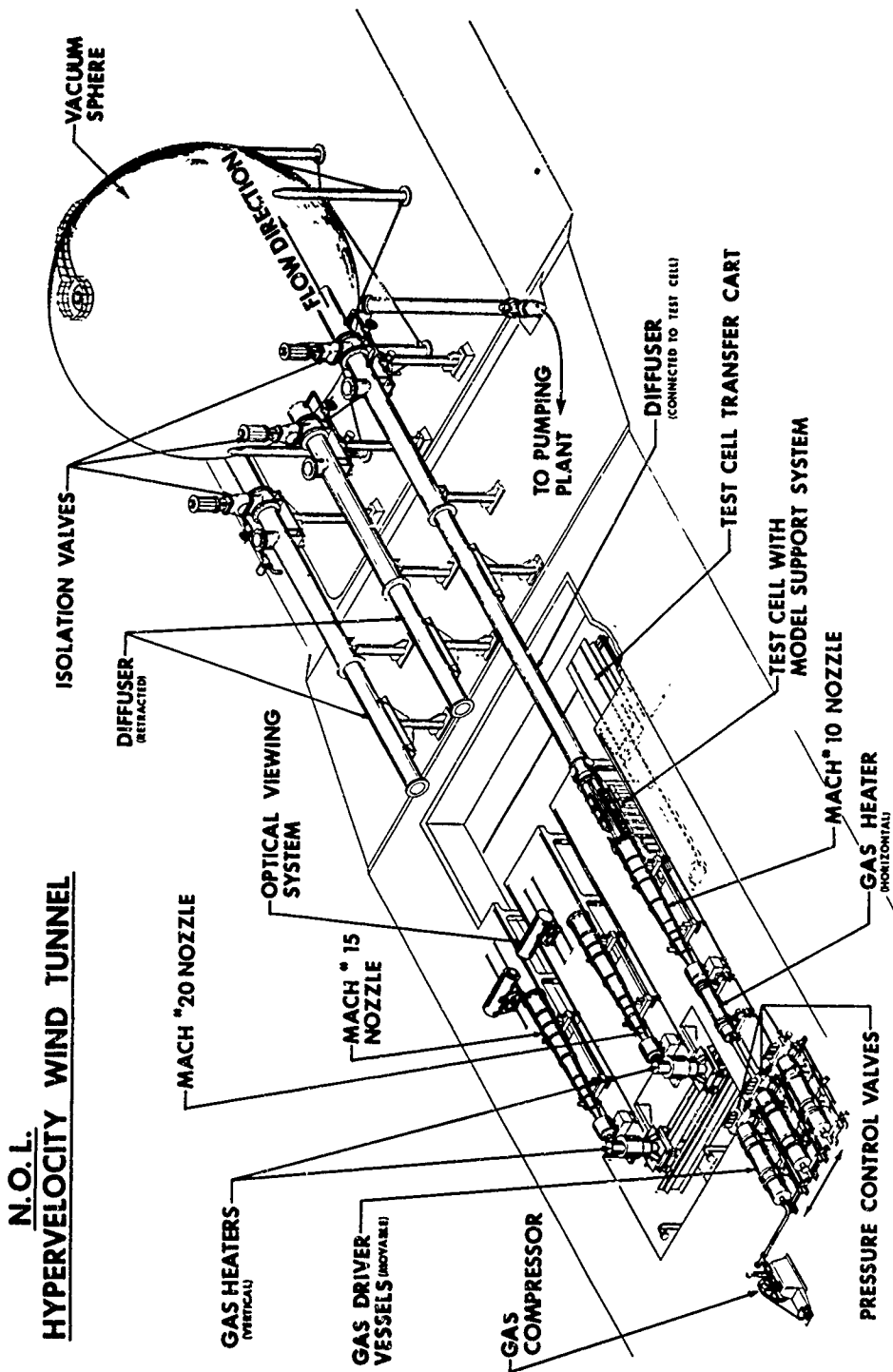


FIGURE 4 REQUIRED SUPPLY PRESSURE, CORE DIAMETER, AND VOLUME FLOW RATE FOR GIVEN RED_c AND MASS FLOW RATE (MACH 20)



N.O.L.
HYPERVELOCITY WIND TUNNEL

FIGURE 5 CUTAWAY VIEW OF TUNNEL SYSTEM

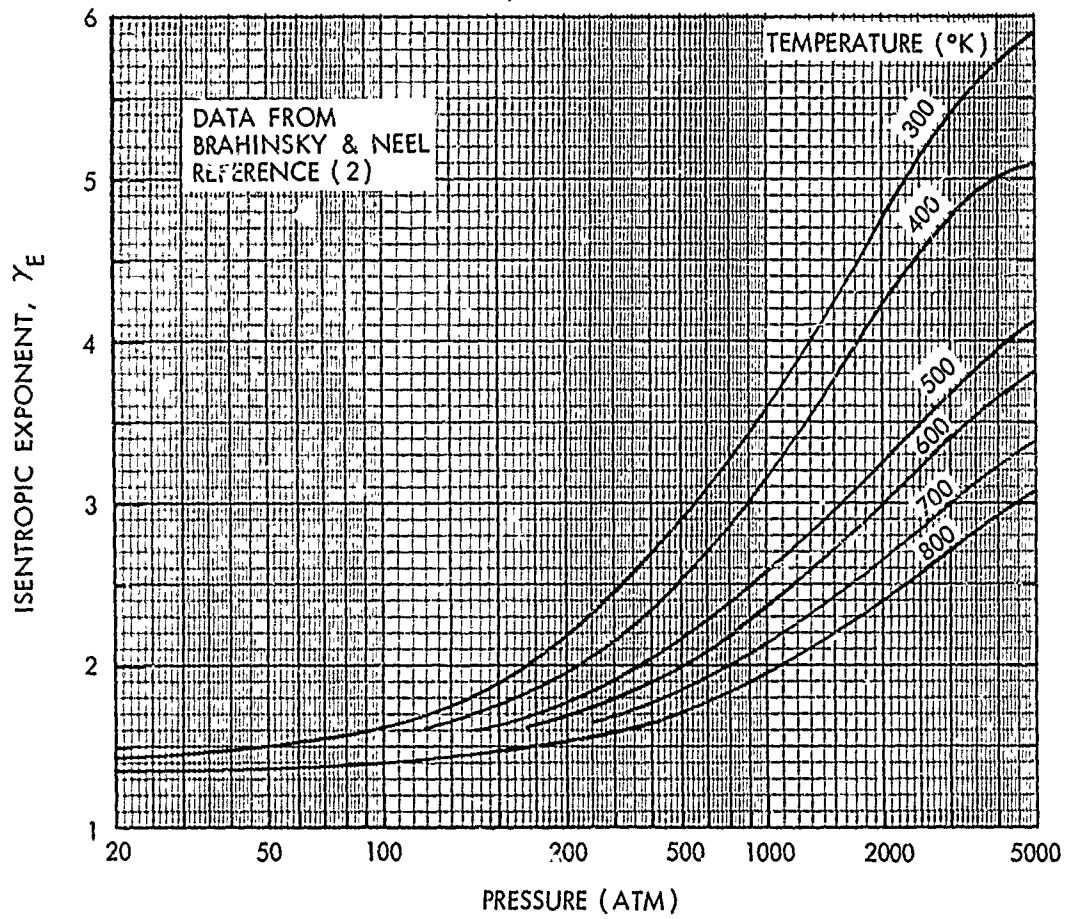


FIGURE 6 VARIATION OF ISENTROPIC EXPONENT WITH PRESSURE AND TEMPERATURE

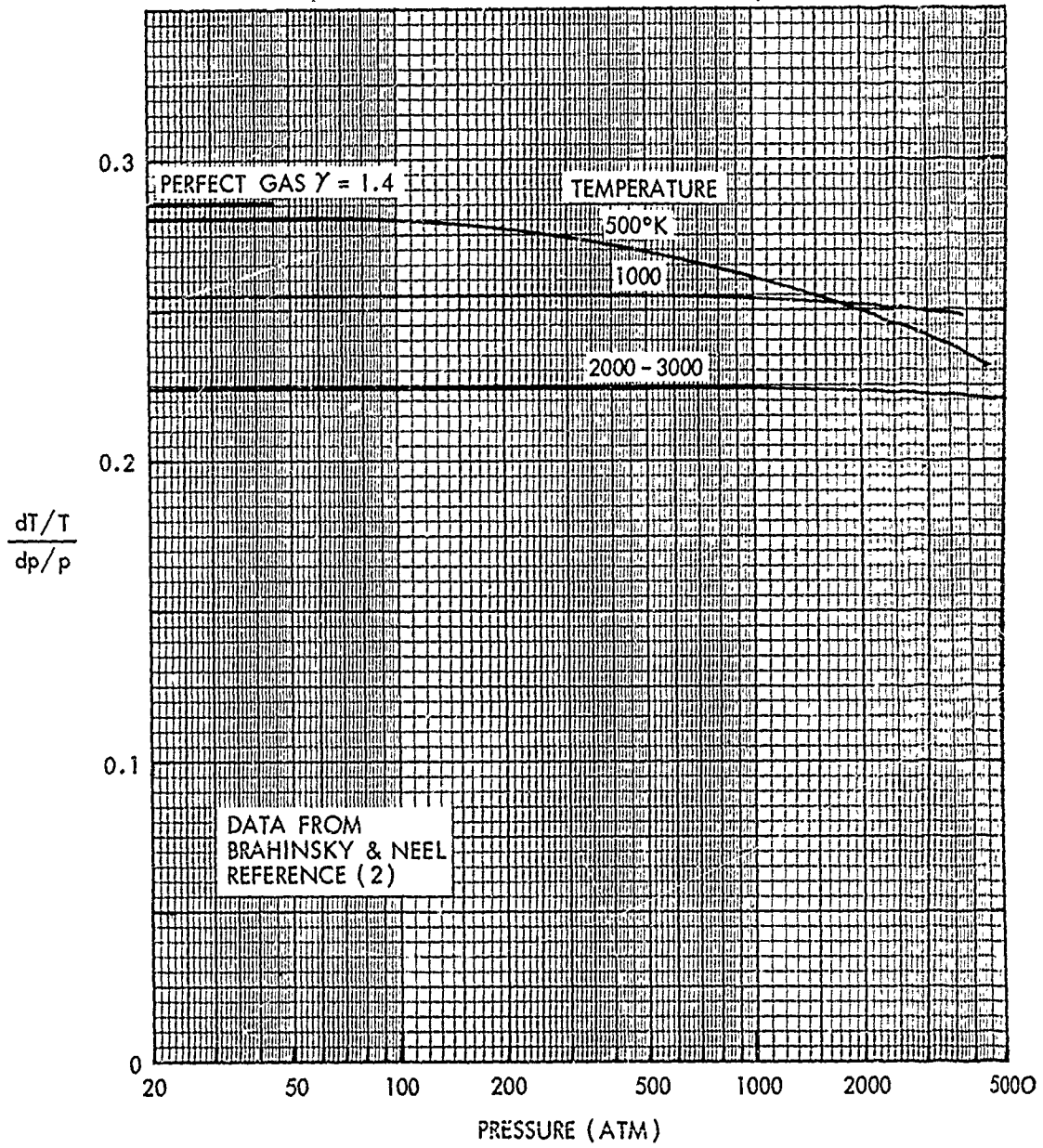


FIGURE 7 RATIO OF TEMPERATURE CHANGES TO PRESSURE CHANGES IN HEATER VESSEL DURING RUN WITH OPEN-CLOSED TYPE VALVES

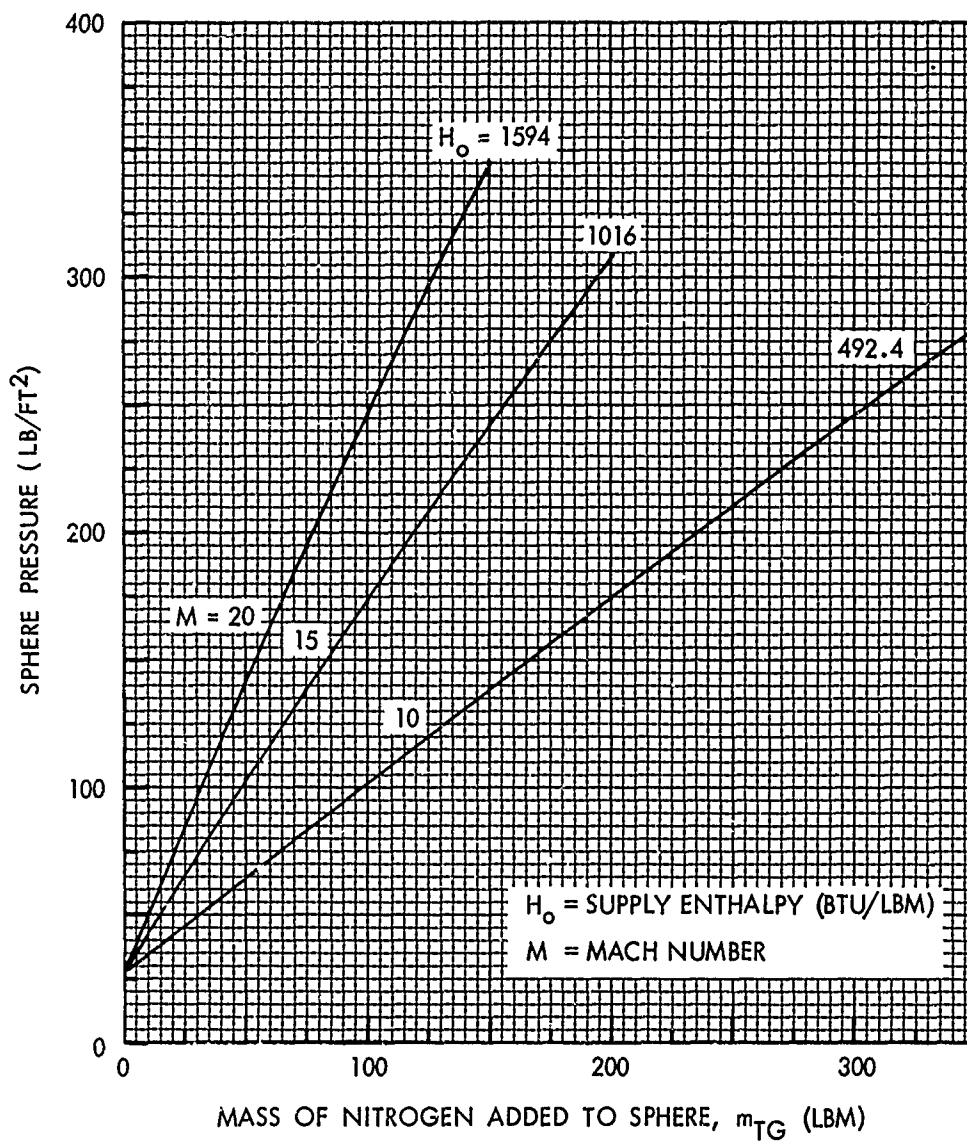


FIGURE 8 PRESSURE RISE IN VACUUM SPHERE DURING TUNNEL OPERATION

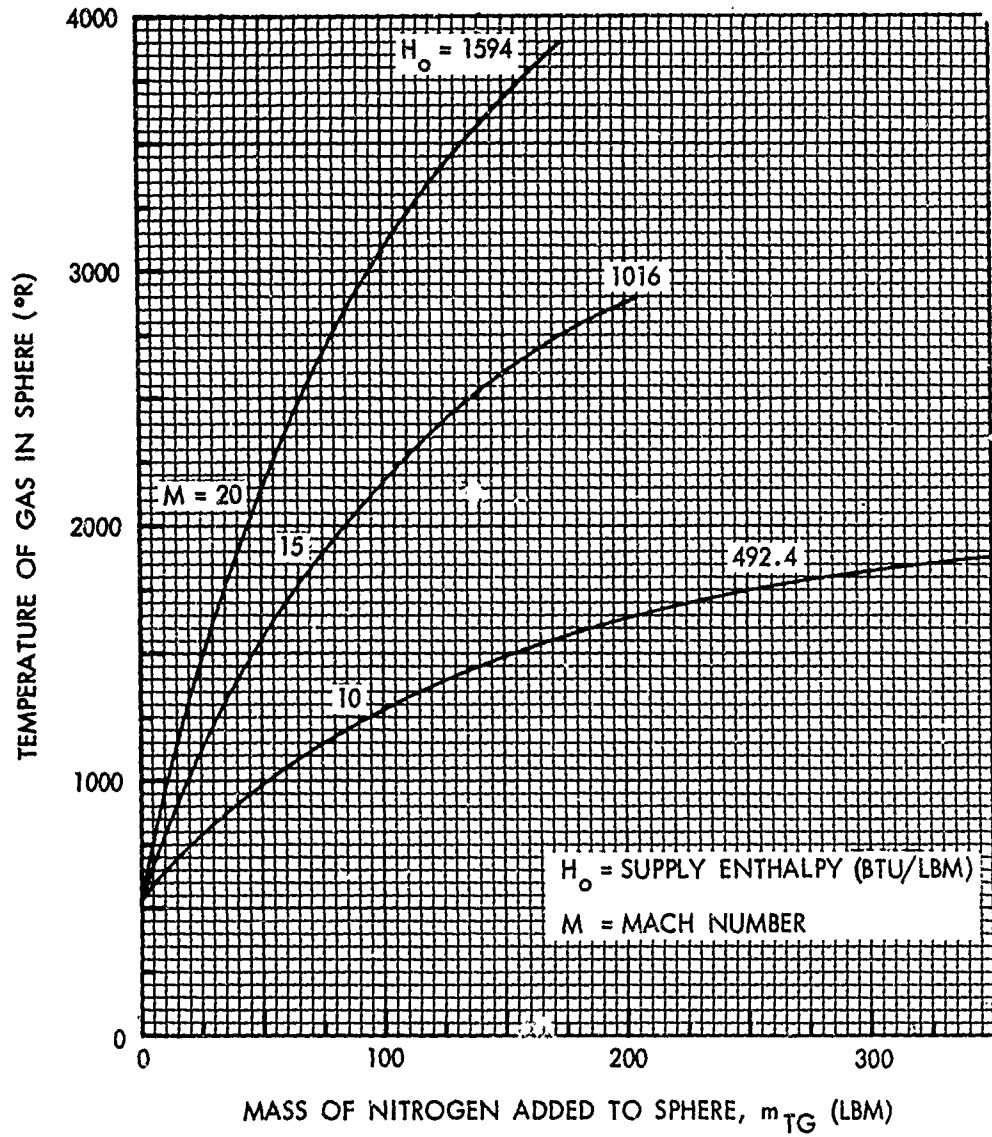


FIGURE 9 TEMPERATURE RISE IN VACUUM SPHERE DURING TUNNEL OPERATION

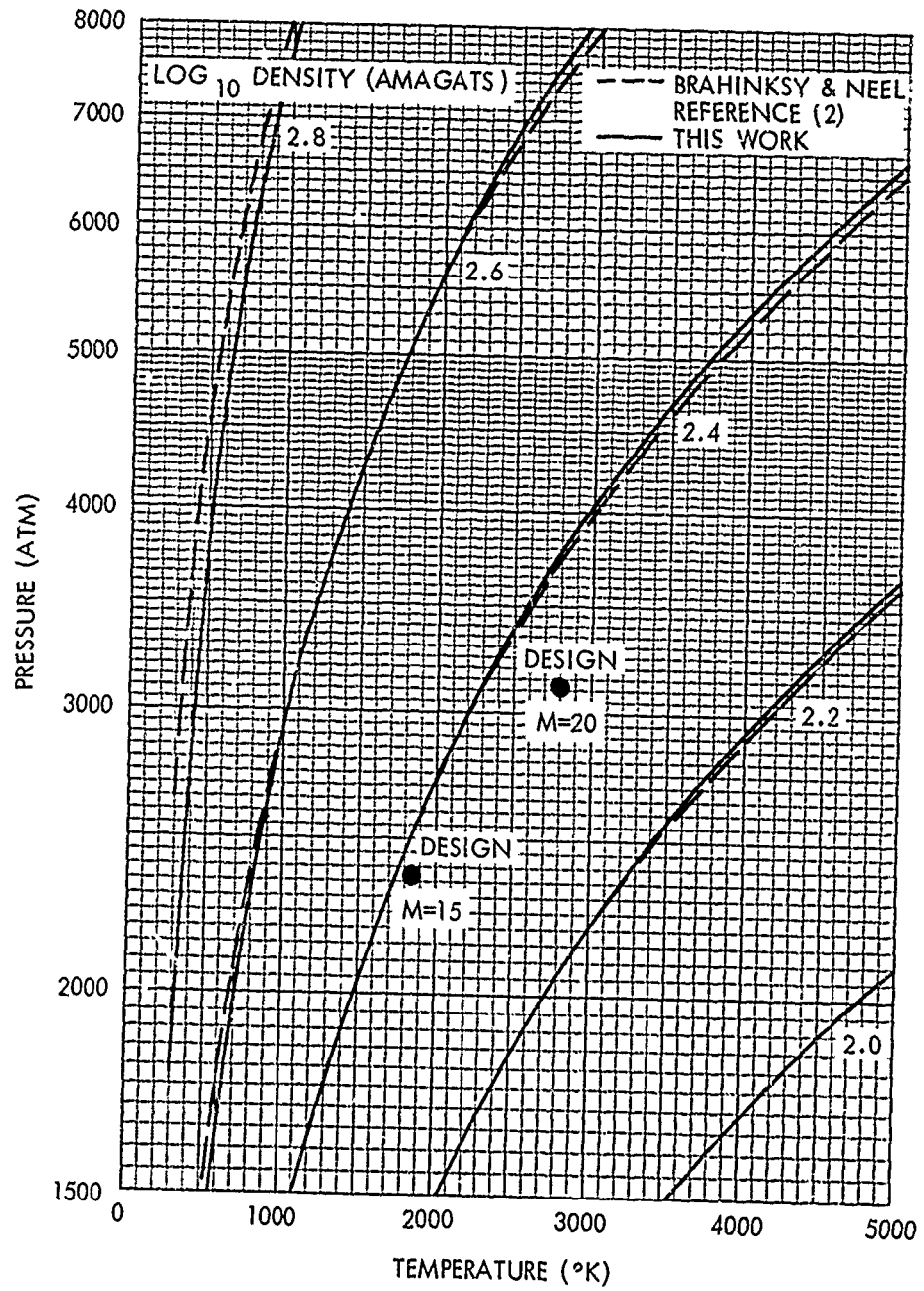


FIGURE 10 COMPARISON OF PRESSURE-TEMPERATURE VARIATIONS AT HIGH DENSITIES WITH AEDC DATA TABULATIONS

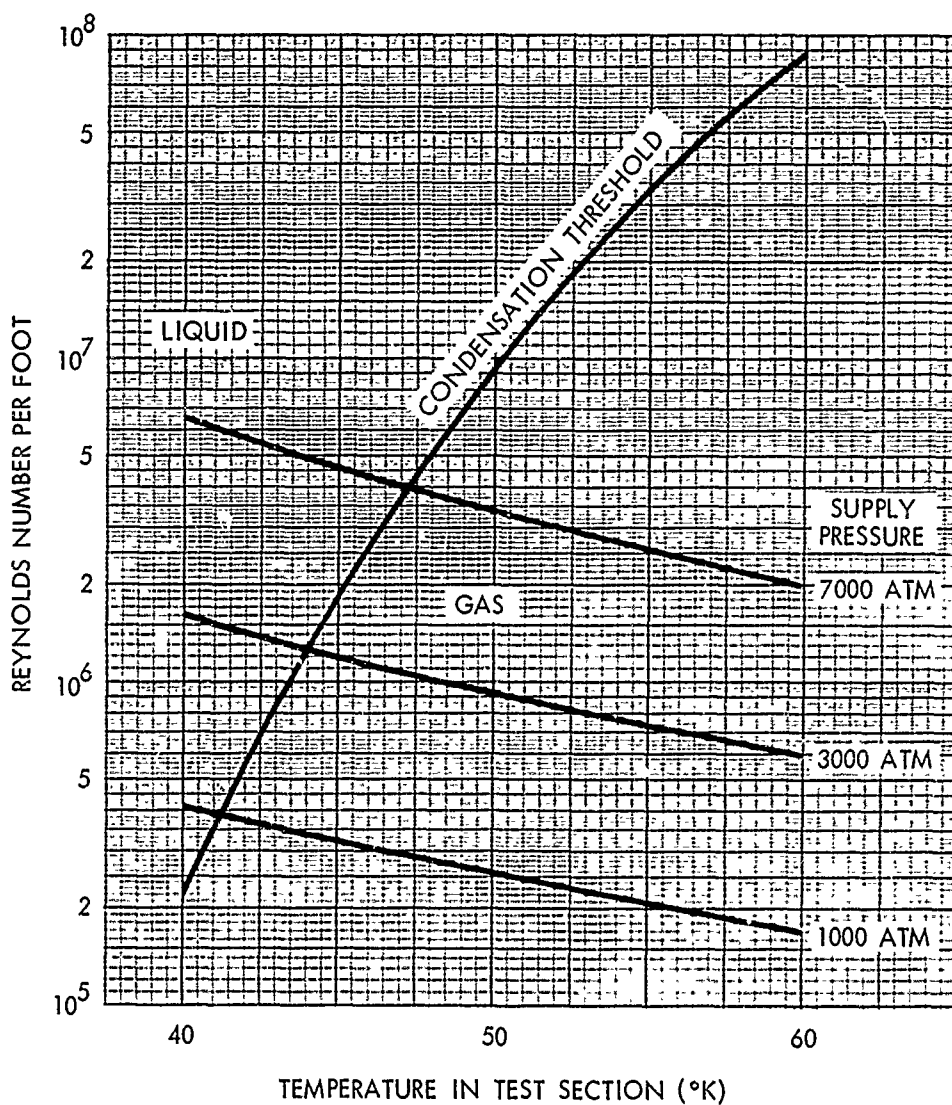


FIGURE 11 VARIATION OF REYNOLDS NUMBER IN TEST SECTION WITH TEMPERATURE FOR CONSTANT PRESSURE OR CONDENSATION THRESHOLD OPERATION AT MACH 20

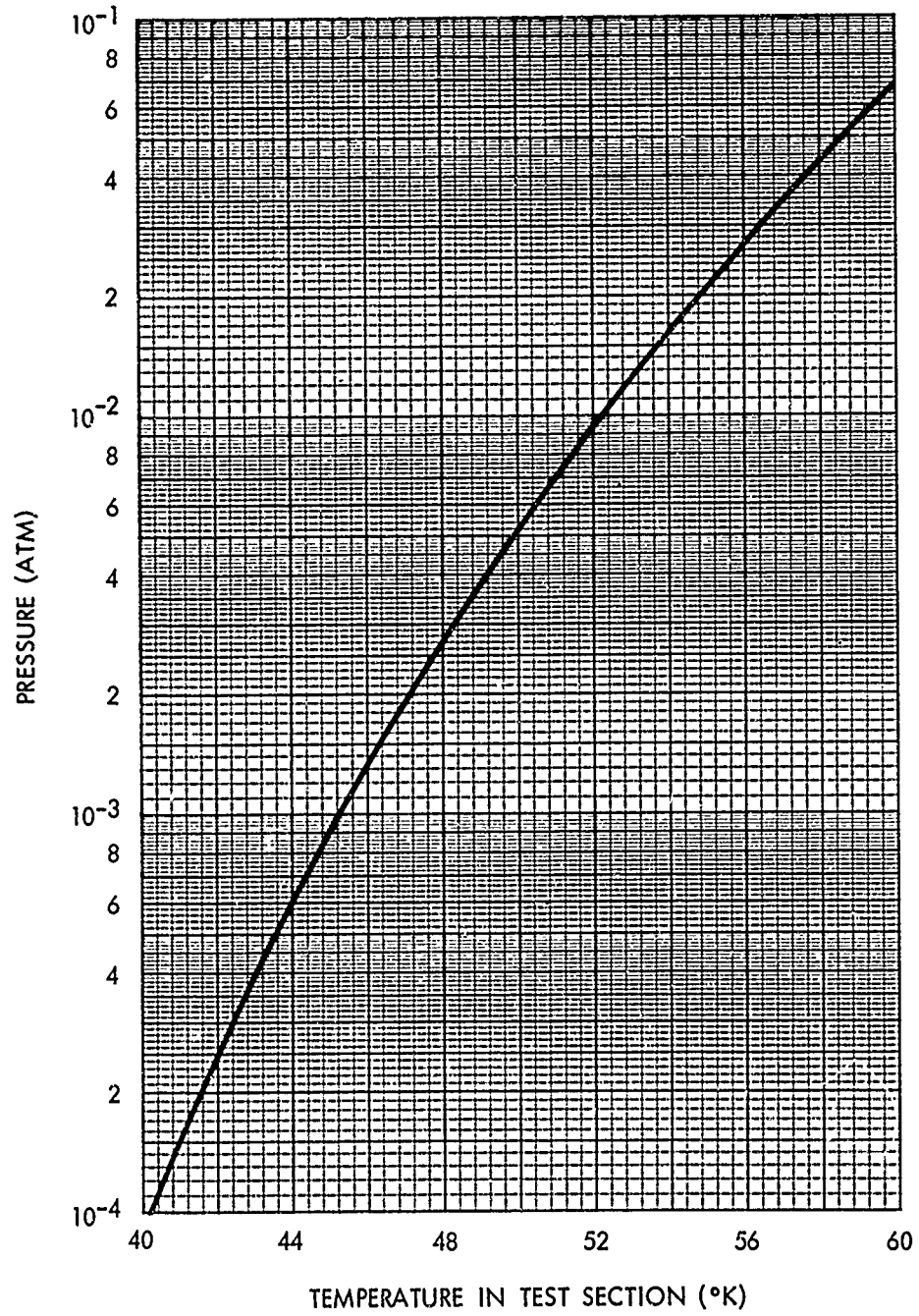


FIGURE 12 VARIATION OF PRESSURE IN TEST SECTION WITH TEMPERATURE FOR CONDENSATION THRESHOLD OPERATION

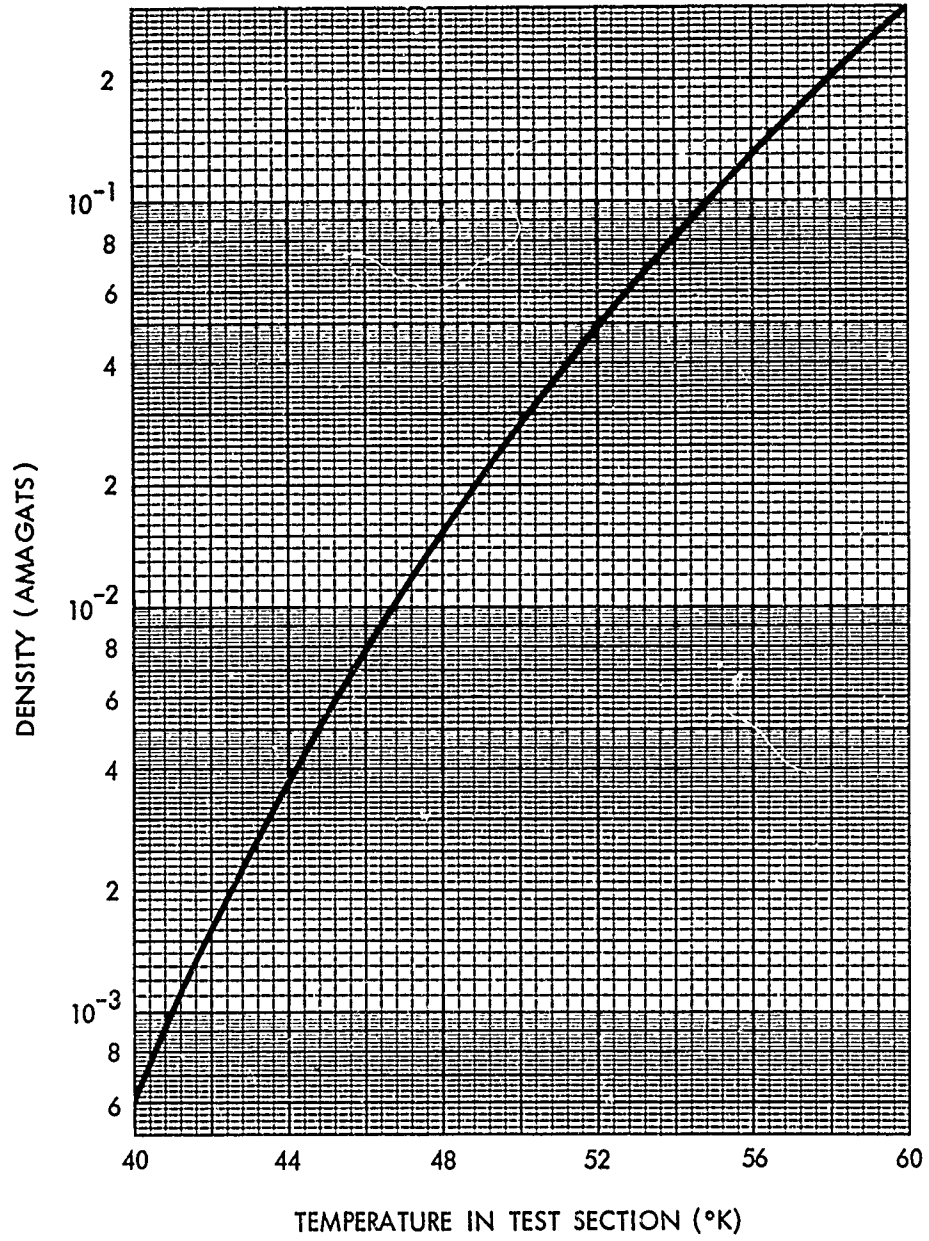


FIGURE 13 VARIATION OF DENSITY IN TEST SECTION WITH TEMPERATURE FOR CONDENSATION THRESHOLD OPERATION

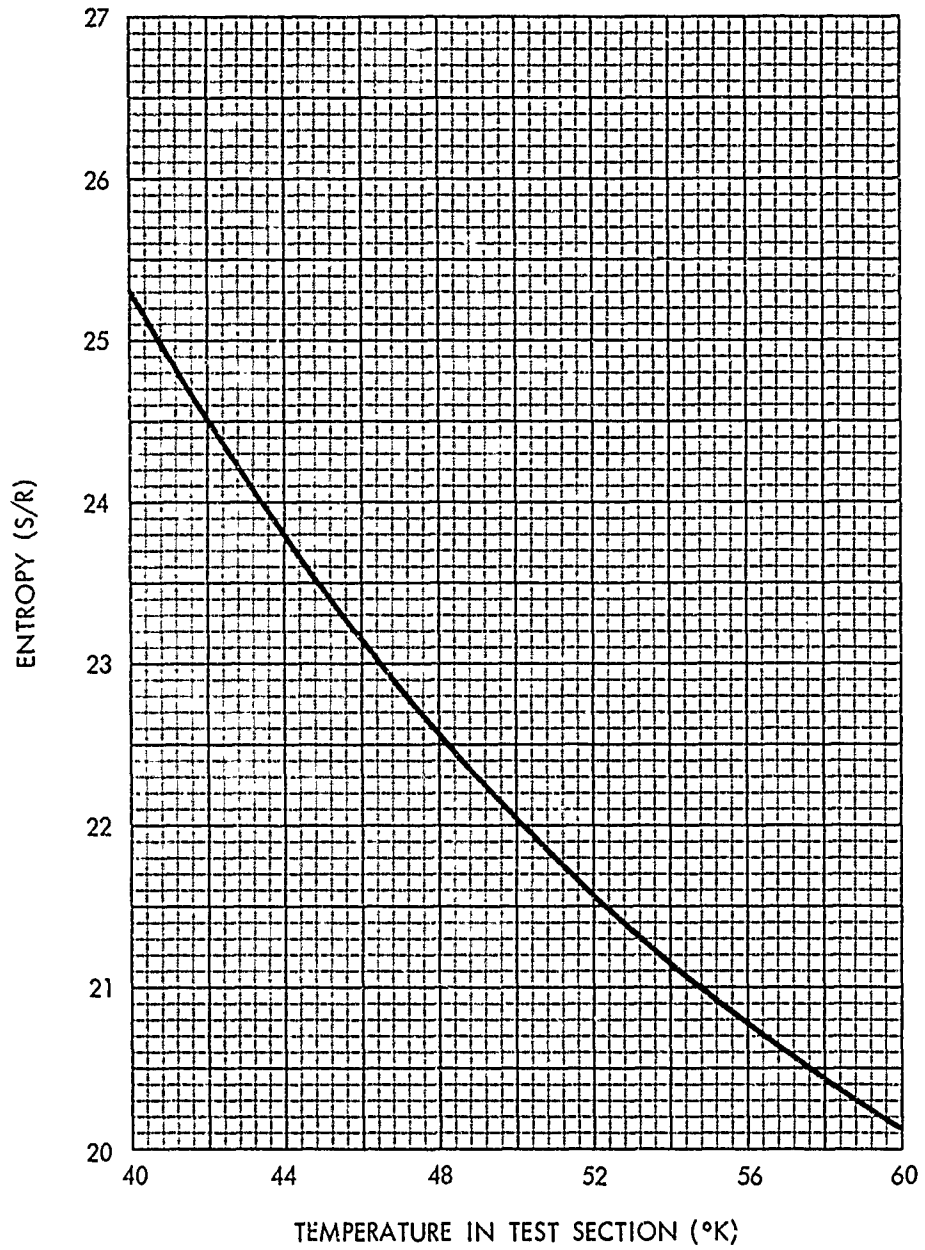


FIGURE 14 VARIATION OF ENTROPY IN TEST SECTION WITH TEMPERATURE FOR CONDENSATION THRESHOLD OPERATION

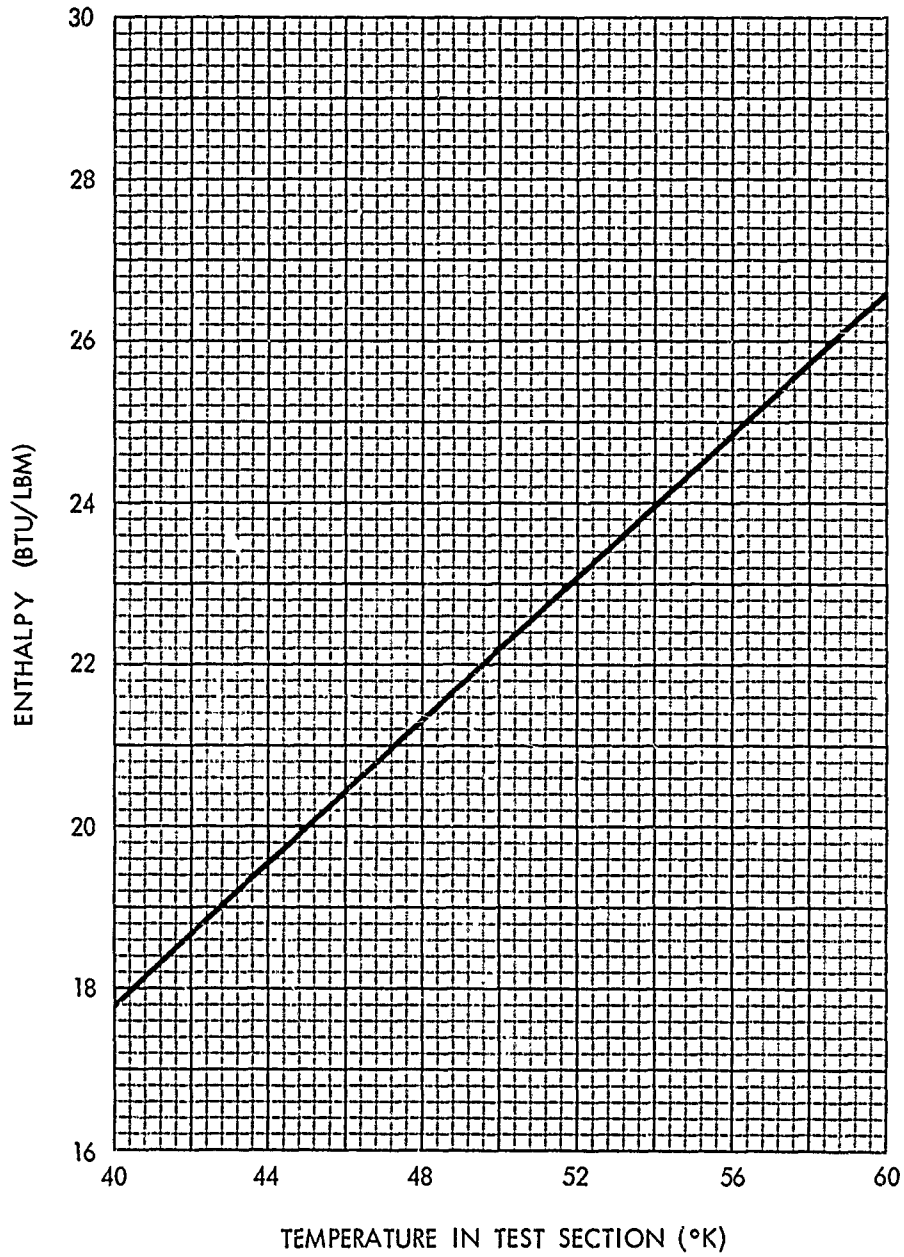


FIGURE 15 VARIATION OF ENTHALPY IN TEST SECTION WITH TEMPERATURE FOR CONDENSATION THRESHOLD OPERATION

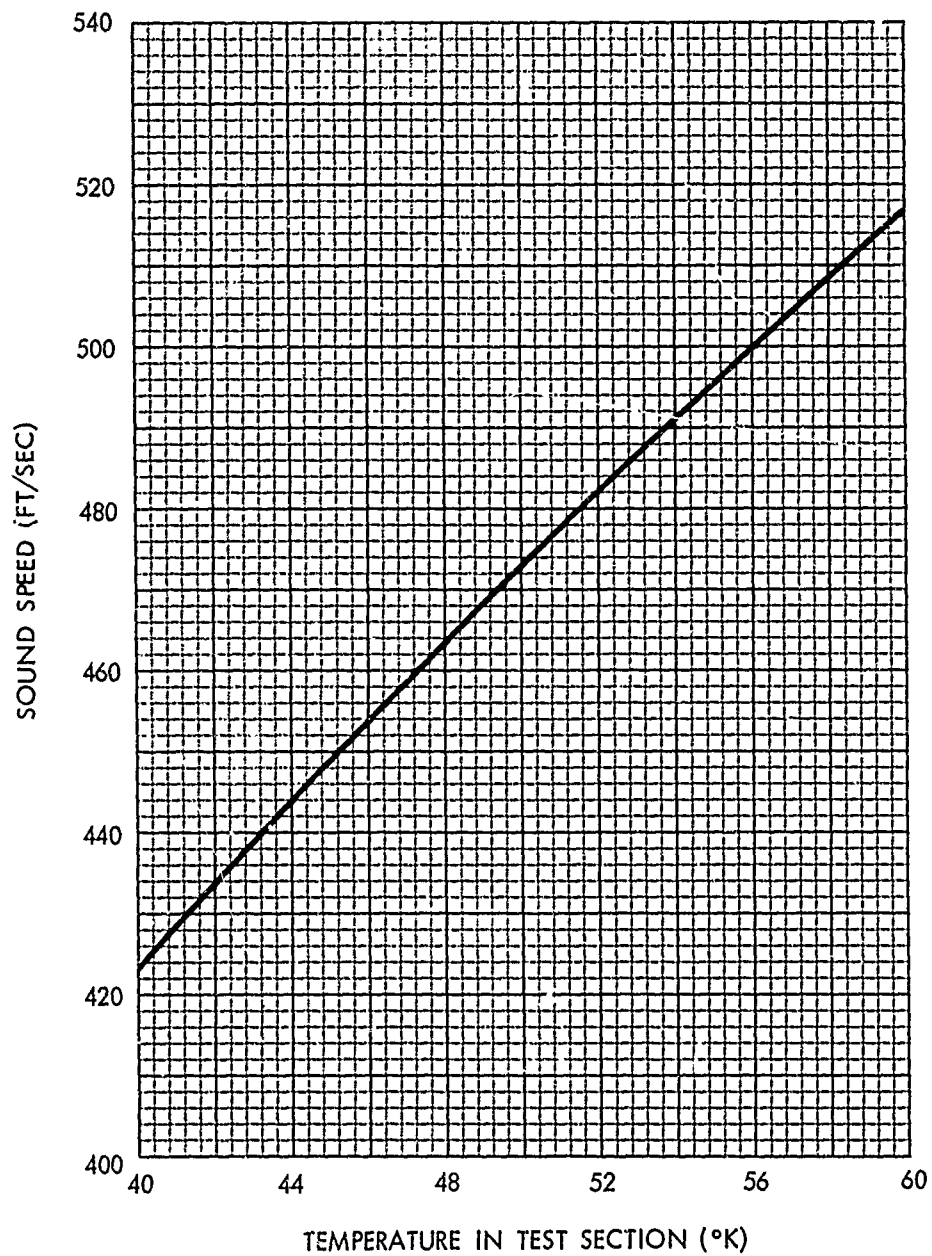


FIGURE 16 VARIATION OF SOUND SPEED IN TEST SECTION WITH TEMPERATURE FOR CONDENSATION THRESHOLD OPERATION

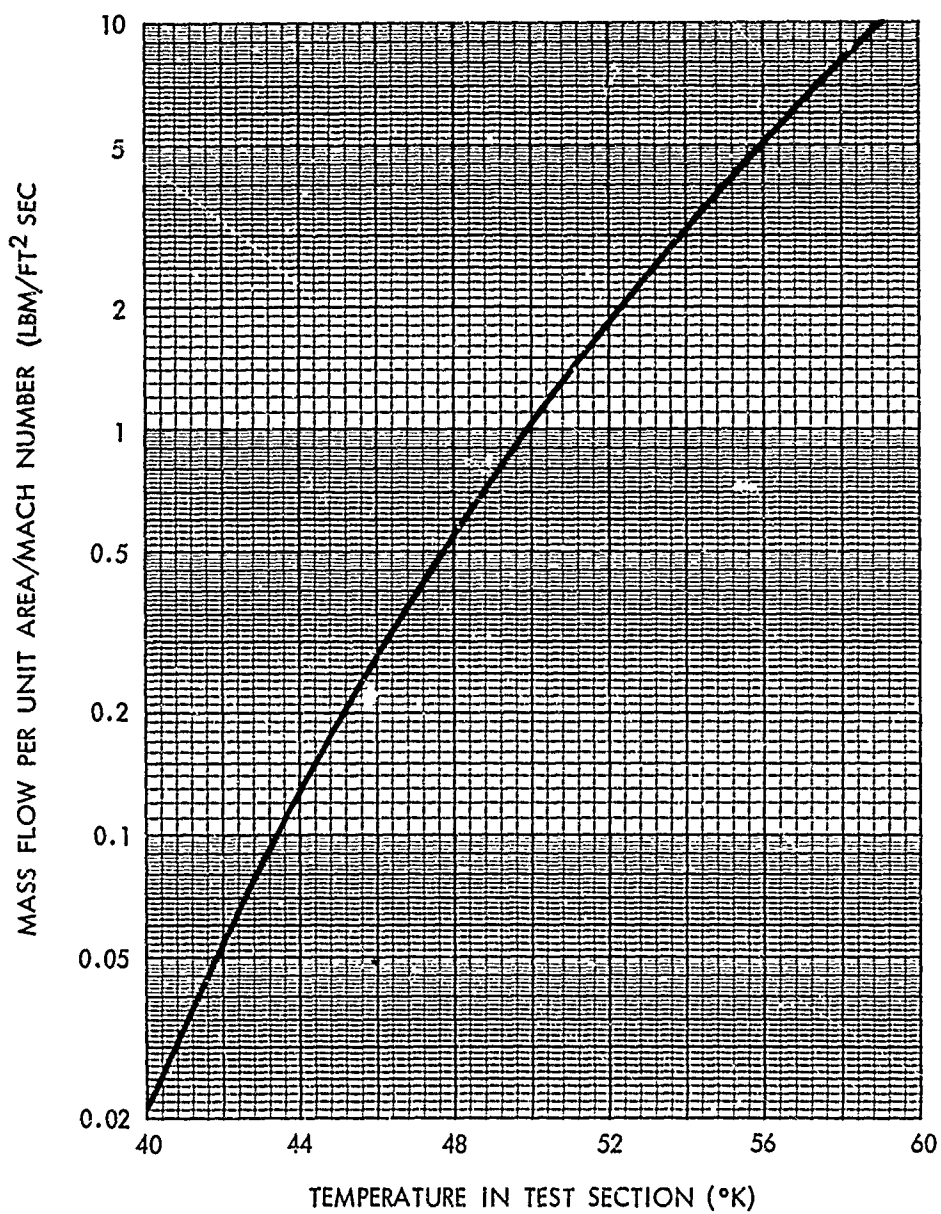


FIGURE 17 VARIATION OF MASS FLOW IN TEST SECTION WITH TEMPERATURE FOR CONDENSATION THRESHOLD OPERATION

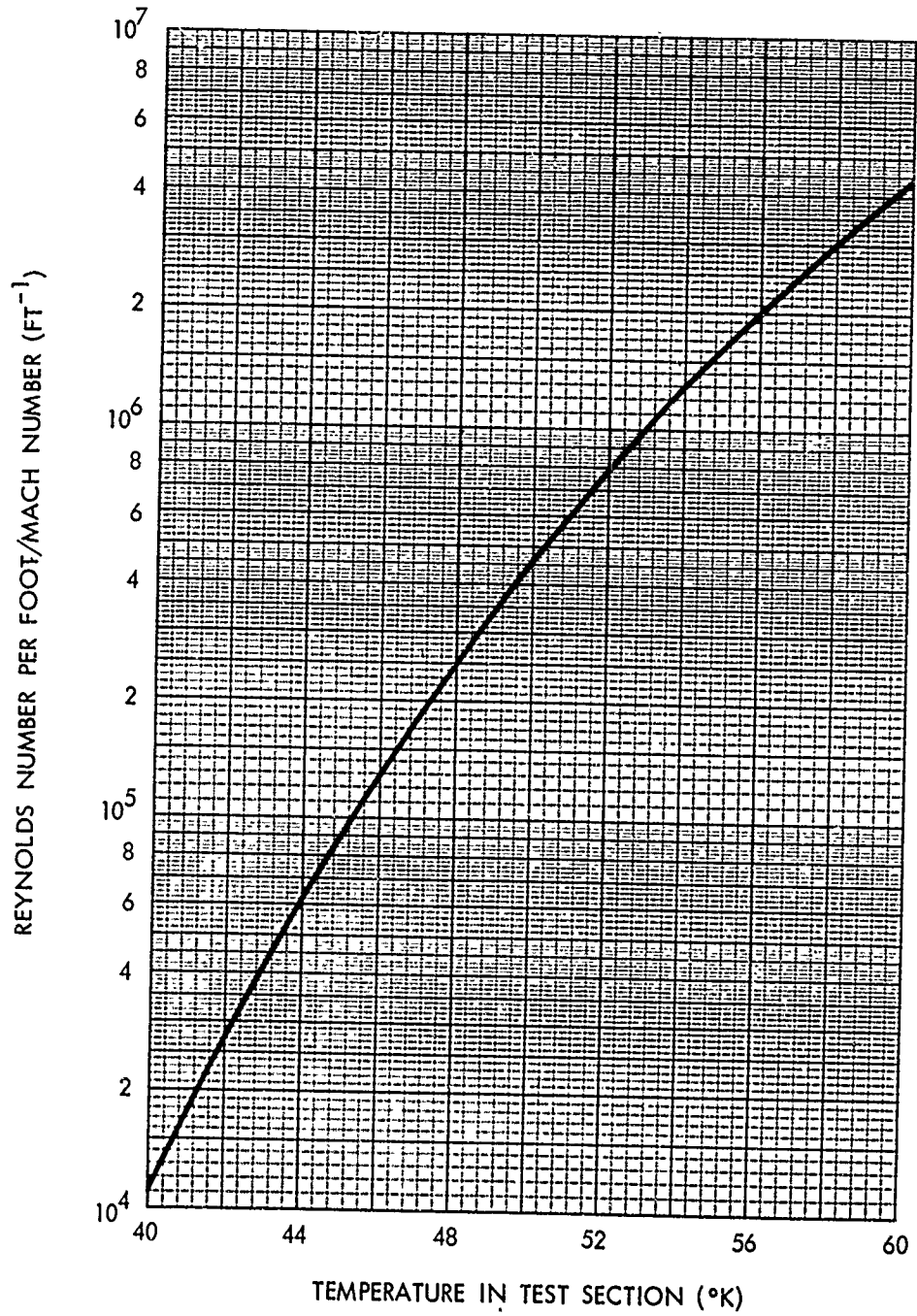


FIGURE 18 VARIATION OF REYNOLDS NUMBER IN TEST SECTION WITH TEMPERATURE FOR CONDENSATION THRESHOLD OPERATION

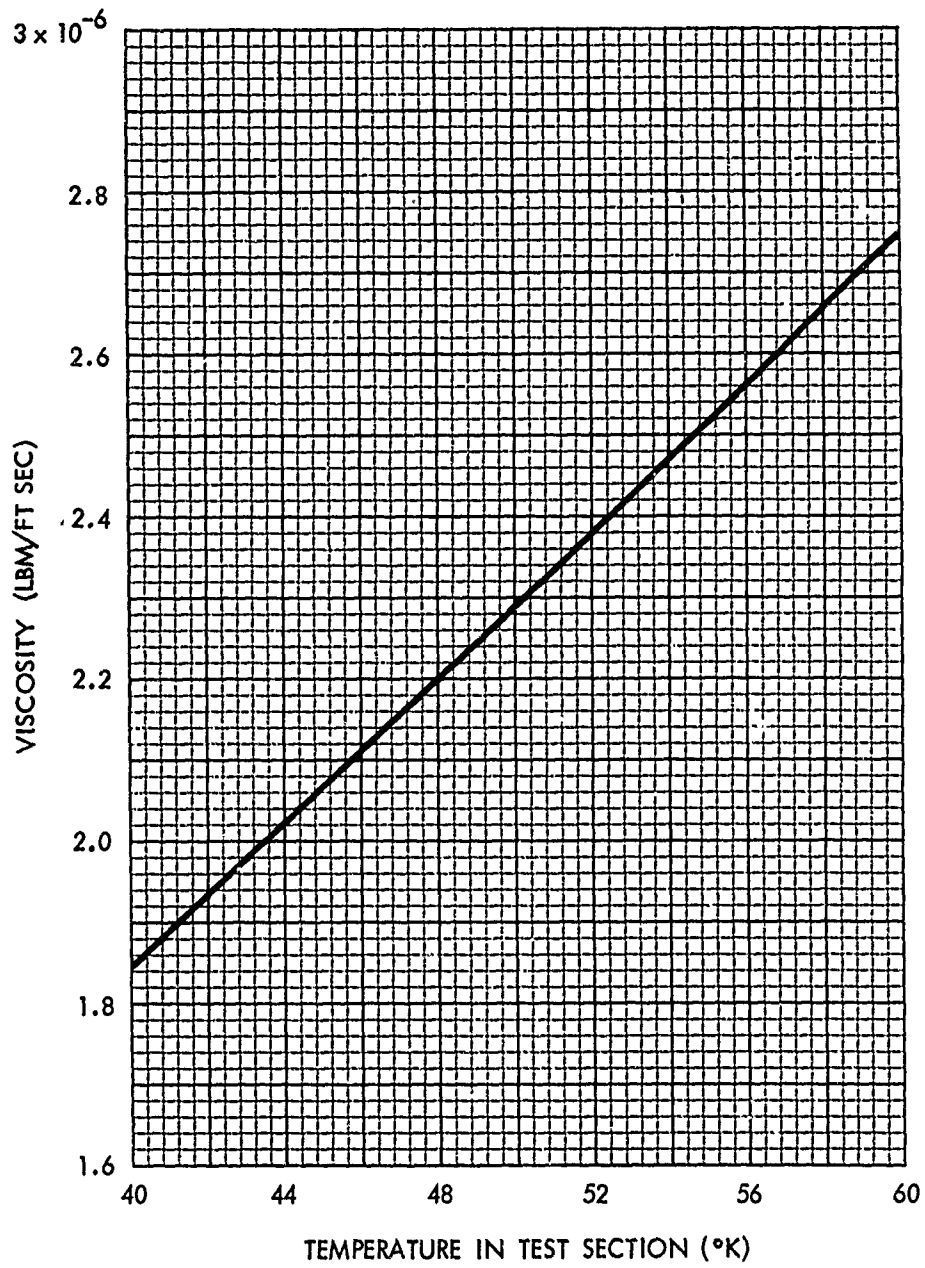


FIGURE 19 VARIATION OF VISCOSITY IN TEST SECTION WITH TEMPERATURE FOR CONDENSATION THRESHOLD OPERATION

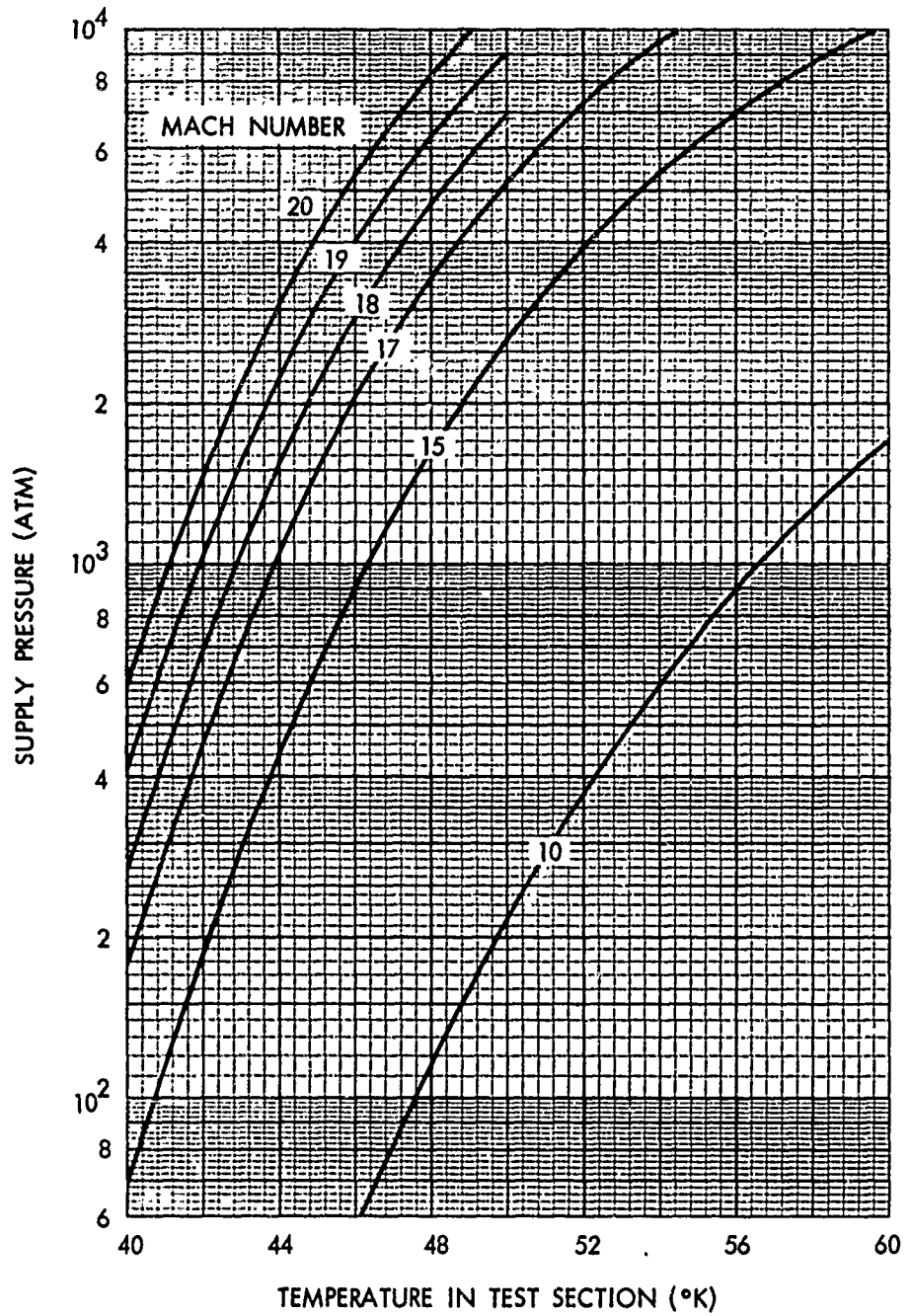


FIGURE 20 VARIATION OF SUPPLY PRESSURE REQUIRED FOR CONDENSATION THRESHOLD OPERATION WITH TEST SECTION TEMPERATURE AND MACH NUMBER

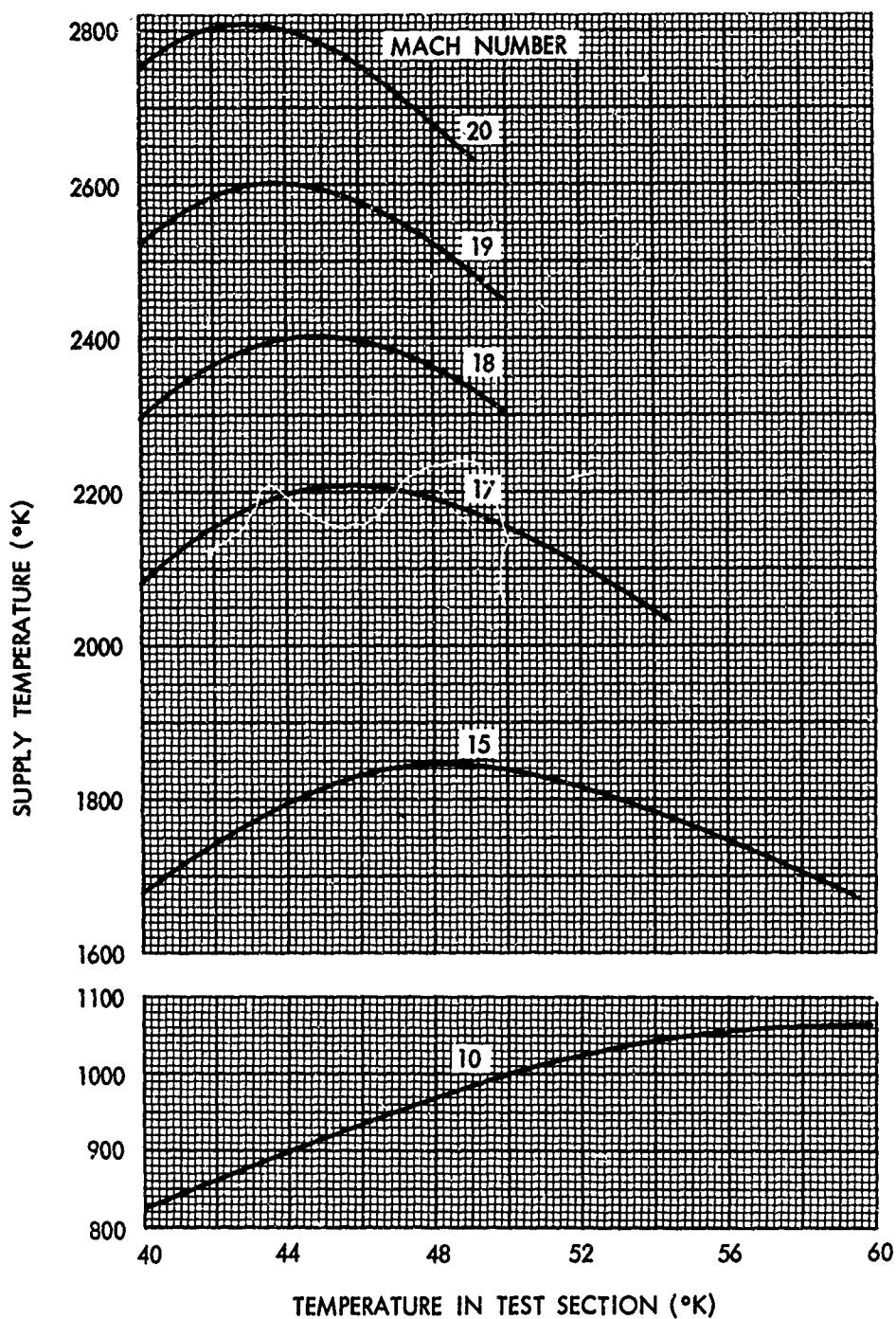


FIGURE 21 VARIATION OF SUPPLY TEMPERATURE REQUIRED FOR CONDENSATION THRESHOLD OPERATION WITH TEST SECTION TEMPERATURE AND MACH NUMBER

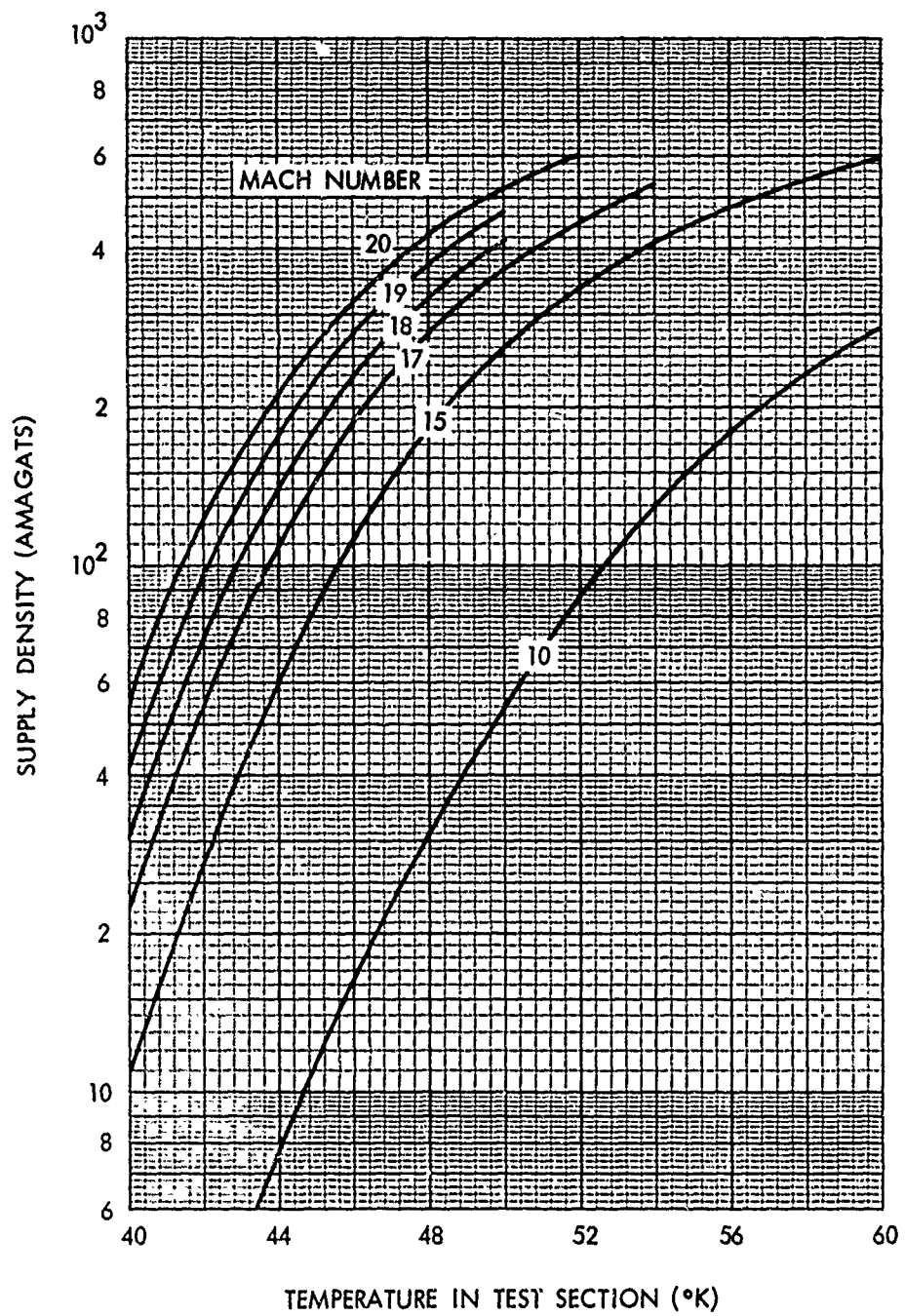


FIGURE 22 VARIATION OF SUPPLY DENSITY REQUIRED FOR CONDENSATION THRESHOLD OPERATION WITH TEST SECTION TEMPERATURE AND MACH NUMBER

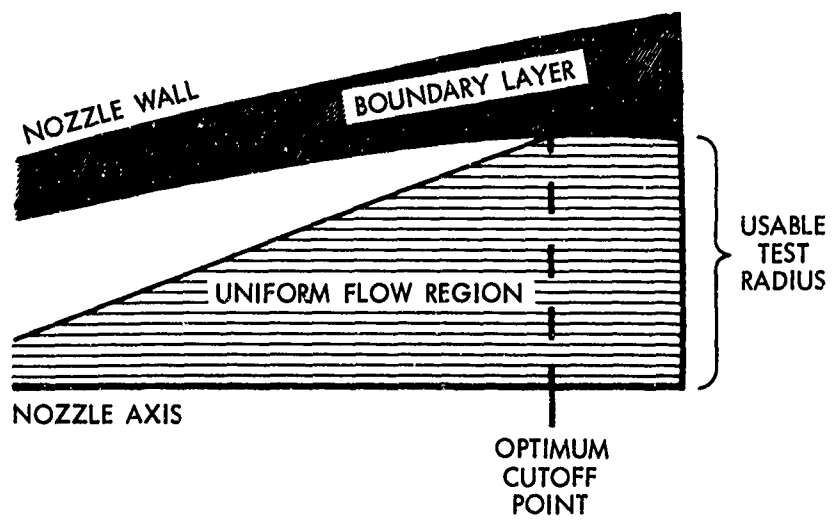


FIGURE 23 SCHEMATIC DIAGRAM OF NOZZLE EXIT SHOWING DEFINITION AND LOCATION OF OPTIMUM CUTOFF POINT